BIOMECHANICAL PROPERTIES OF EXPANDED SHEEP SKIN

NUR AINI SABRIN BINTI MANSSOR
@ SHUKRI

DISSERTATION SUBMITTED IN FULFILMENT
OF THE REQUIREMENT FOR THE DEGREE OF
MASTER OF BIOMEDICAL ENGINEERING

FACULTY OF ENGINEERING
UNIVERSITY OF MALAYA
KUALA LUMPUR

2014

Abstract

Tissue expansion provides extra tissue which is useful for surgical reconstruction field and had been utilized since ages ago. Tissue expansion using self-inflating tissue expander had made its breakthrough in recent years. However similar issue arises whether the quality of tissue produced is comparable with original tissue. Therefore, the objectives of this study were to investigate the surface topography and elastic properties of expanded skin tissue at the macro and ultrastructural levels. Two groups of five adult male Dorper sheep were used in the study. One group acted as the control group and the other was implanted subcutaneously with cylindrical 20 x 5 mm osmotic tissue expanders at the lower limb region, and allowed to reach equilibrium, and harvested. The surface roughness and elastic modulus analysis were carried out using the Alicona 3D Optical Analyzer and BioAFM. The force spectroscopy test was performed on collagen fibrils at 10 points. In a separate set of experiments, samples from both groups were subjected to uniaxial tensile test and the elastic moduli at initial region (E_0) and linear terminal region (E_∞) as well as the limit strain were obtained. The average surface roughness (0.55 ± 0.27 μm) was significantly ($p<0.05$) lower in the expanded group (1.42 ± 0.64 μm). It was observed that the collagen fibrils in the expanded tissues were thinner. The modulus of the collagen fibrils in the expanded skin was 45.9 ± 24 MPa whereas the modulus of collagen fibrils in normal skin was 36.1 ± 29.5 MPa with no significant difference ($p >0.05$). As for the tensiometric parameters tested on bulk skin tissue, the E_0 are 0.27 ± 0.19 MPa and 0.85 ± 0.67 MPa for normal and expanded skin, respectively. The E_∞ obtained for normal and expanded groups are 2.14 ± 1.46 MPa and 4.4 ± 1.97 MPa, respectively. The limit strain for expanded skin is lower (0.3 ± 0.2)

compared to normal skin (0.50 ± 0.16). The surface topography of the expanded skin shows evidence of fibers being stretched; therefore it affects the resting tension of the collagen fibrils, thus producing slightly higher elastic modulus of expanded skin and fibrils. However, from these experiments it was not possible to prove a possibility of new tissue generation in expanded skin because it requires concurrent histological experiments.

Abstrak

Pengembangan tisu tambahan yang meluas digunakan dalam bidang pembedahan pembinaan semula telah digunakan sejak zaman dahulu. Perkembangan tisu menggunakan diri menaikkan penambah tisu telah mencapai kemajuan besar dalam tahun-tahun kebelakangan ini. Walau bagaimanapun isu yang sama timbul sama ada kualiti tisu yang dihasilkan setanding dengan tisu asal. Objektif kajian ini adalah untuk mengkaji topografi permukaan dan sifat-sifat elastik perkembangan tisu kulit di peringkat makro dan ultrastruktural . Dua kumpulan biri-biri jantan dari jenis Dorper telah digunakan dalam kajian ini. Satu kumpulan sebagai kumpulan kawalan dan yang satu lagi telah diimplan dengan pengembang tisu silinder bersaiz 20 x 5 mm di kaki binatang kajian tersebut dan dibiarkan berkembang sehingga mencapai keseimbangan, dan dikeluarkan. Kekasaran permukaan dan analisis modulus elastik telah dijalankan menggunakan Alicona 3D optik Analyzer dan BioAFM . Ujian spektroskopi telah dijalankan ke atas fiber kolagen pada 10 tempat. Dalam eksperimen yang berlainan, sampel dari kedua-dua kumpulan telah dikenakan ujian tegangan dan modulus elastik di bahagian permulaan (E0) dan bahagian terminal linear ($E \infty$) dan juga keterikan had diperoleh. Purata kekasaran permukaan (0.55 ± 0.27 μm) adalah ($p < 0.05$) lebih rendah dalam tisu yang mengembang (1.42 ± 0.64 μm). Diperhatikan bahawa fiber kolagen dalam tisu berkembang lebih nipis. Modulus fiber kolagen dalam kulit berkembang ialah 45.9 ± 24 MPa manakala modulus fiber kolagen dalam kulit normal ialah 36.1 ± 29.5 MPa dengan tiada perbezaan signifikan ($p> 0.05$). Bagi parameter tensiometrik yang diuji ke atas tisu kulit untuk kulit normal dan berkembang masing-masing adalah E0 ialah 0.27 ± 0.19 MPa dan 0.85 ± 0.67 MPa.

Modulus terminal E_∞ diperoleh untuk kumpulan normal dan berkembang ialah 2.14 ± 1.46 MPa dan 4.4 ± 1.97 MPa, masing-masing. Had tegangan untuk kulit normal lebih tinggi (0.5 ± 0.16) berbanding dengan kulit kembang (0.3 ± 0.20). Topografi permukaan kulit berkembang menunjukkan bukti fiber telah menegang; dan memberi kesan kepada ketegangan rehat fiber kolagen, dengan itu menghasilkan modulus elastik yang lebih tinggi daripada kulit berkembang. Walau bagaimanapun, eksperimen ini tidak memungkinkan untuk membuktikan kemungkinan pertumbuhan tisu baru di dalam kulit berkembang kerana ia memerlukan ujikaji histologi.

Acknowledgement

First and foremost I am grateful to the Merciful God for giving me His bless by giving me the opportunity to register as a postgraduate student in the University Malaya at the MEng of Biomedical Engineering programme. During the period of conducting my research and writing this report, I am thankful to Him for giving me good health. Besides, I realize that there are many people and institutions that supported me in many ways, for without them, I am not able to finish my research project.

First of all, I would like to thank my parents for their endless support during this period. The same goes for my siblings who never let me give up in my study.

I am deeply grateful for my supervisor Prof. Dr. Ir. Wan Abu Bakar Wan Abas for his guidance and help in completing this research and report. He gave me a lot of freedom to work in my own way, and a lot of information which is quite hard for me to understand without his help. Besides, I really appreciate his time spent with me to discuss things I do not understand amidst his busy schedule.

I owe many thanks to my co-supervisor, Prof Zamri Radzi for giving me the chance to be part of the 'Tissue Expander team' in the Faculty of Dentistry, UM. I gained a lot of wonderful experiences dealing with sheep, and working with AFM. I appreciate his daily supervision and his willingness to spend time with me whenever I would call for discussion.

I would like to express my gratitude to Dr. Philip Liu from JPK Instrument, Singapore for guiding me through and answering my questions without fail, regarding AFM. I would like to thank Dr. Abd. Razaq, for helping me understand more on the behaviour of skin and correct me when I make mistakes. Thank you very much to my colleagues in the Tissue Expander group for continuosly cheering and supporting me during my research. Thank you for your information and discussion in their study for giving me the opportunity to understand more about this research.

I thank the University Malaya for giving the opportunity to use a very high-tech equipment such as AFM in order for me to complete this research. Besides, I owe my gratitude to the Faculty of Veterinery, Universiti Putra Malaysia, for providing us with their best hospitality for us to conduct surgery (implantation and explantation) at their site.

Table of Contents

List of Figures

List of Tables

List of Appendixes

List of Symbols and Abbreviations

Atomic Force Microscopy	**AFM**
Force Spectroscopy	FS
Micrometer	μm
Nano meter	nm
Mega Pascal	MPa
Nano Newton	nN
Optimum Cutting Temperature	OCT
phosphate buffer solution	PBS

Chapter 1. INTRODUCTION

1.1. Tissue Expander

Tissue expansion has been first utilized for thousands of years in tribal customs (Bennett and Hirt 1993). In fact, tissue expansion also happens naturally during pregnancy and tumor growth. Skin tissue expansion is a procedure that enables additional tissue to be formed for use in surgical reconstruction. Skin tissue expansion is a procedure that enables additional tissue to be formed for use in surgical reconstruction. The expansion is accomplished by placing a device called as tissue expander beneath skin and let the expander stretched the skin by means of step expansion or continuous expansion. Neumann first introduced the use of tissue expander in clinical field in 1957 by inserting rubber implant subcutaneously to reconstruct external ear deformity (Neumann, 1957). Since that time, the devices have been improved to silastic inflatable balloons and widely used in current clinical practice (Figure 1.1). A conventional tissue expander consists of silicone pouches with injection ports which is integrated in implant or connected by tubing. Step expansion is employed by injecting saline into the port periodically. As the three-dimensional volume of the implant increases, tension is placed on the surrounding tissues, resulting in their expansion over time. The major disadvantages of this devise are its bulky size and painful experiences during the course of expansion which is unbearable for some individuals such as children.

topography of surfaces. As a force sensor and nanoindentor AFM can directly measure properties such as the Young's modulus of surfaces.

1.4. Objective

It is the aim of this study to explore the mechanical behaviour of sheep's skin expanded by self-inflating anisotropic tissue expander at macroscale and ultrastructural level and compare the parameters with the normal skin. Present study will be focusing on the elastic property of collagen fibrils and skin tissue. To achieve this aim, the elastic modulus of skin will be determined by performing uniaxial tensile test on skin tissue and the mechanical properties of the collagen fibrils will measured using AFM force spectroscopy. Initial modulus and terminal modulus obtained from initial slope and linear region slope of stress-strain respectively will be determined in order to study about the mechanical behaviour of skin tissue while in a separate set of experiment, elastic modulus (Young's modulus) of several collagen fibrils will be analysed to explore the mechanical behaviour of expanded skin in nano scale.

1.5. Scope of study

The present study involved with the study of tissue mechanics, where the elastic properties of expanded skin tissue was investigated in the hierarchical fibrils and skin tissue level. In addition, the surface roughness and topography of the expanded skin were examined and compare with those of normal tissue.

1.6. Outline of the report

Chapter 2 present a review of studies previously reported on mechanical testing of skin both normal and expanded in bulk tissue and the approach of using AFM to study the mechanical properties of collagen fibrils. In the next part of this report, the detail of methodology conducted in this research was presented. The method of conducting mechanical testing on collagen fibrils and skin tissue were inspired from literatures reported in Chapter 2. We report on the surface topography studies using Alicona and AFM. Besides, we also conducted mechanical testing on collagen fibrils using AFM and uniaxial tensile test on skin tissue using Instron machine. The results of each experiments and observations are reported in the Chapter 4 of this research. Some of the discussion on the comparison with the literatures and limitation in this study are also reported in this chapter. Chapter 5 reports on the summary and conclusion found from this study.

Chapter 2. LITERATURE REVIEW

2.1. Skin structures

The skin is a soft tissue and its main physiological functions are protection, regulation, and sensation. The mechanical properties of skin are complex because of the complex skin structure. The skin comprises of three main layer, epidermis, dermis and hypodermis. Each layer possesses different properties in order for skin to perform its physiological functions. The outer most layer of the skin is the stratum corneum consisting of nucleated cells. Its specific properties are very dependent on the temperature and relative humidity of the environment (Wildnauer et *al*., 1971, Agache et *al*., 1973, Marks, 2004, Wu et *al*., 2006). The literature reports that, despite performing the tests on different sample site, the mechanical properties are highly dependent on environment. The second layer of the skin is the dermis which makes up the bulk of the human skin. Collagen comprises about 75% of the fat free dry weight and 18-30% of the volume of dermis and forms an irregular network that runs almost parallel to the epidermal surface (Finlay, 1969, McGrath et *al*., 2010). The hypodermis is a fibro fatty layer which is loosely connected to the superficial dermis and located over the body surface (Hendriks, 1969).

Due to the complex cross-sectional of skin, it is very hard to predict the mechanical behavior of the whole skin. Besides, the mechanical properties are not similar for all layers.

Therefore, Wilkes et *al*., (1973) considered dermis as the main contributors of mechanical properties of skin in full thickness.

2.1.1. Hierarchical structures of collagen

The mechanical properties of the dermis is directly associated with the arrangement of its constituents. Collagen type I and type III primarily formed the dermis layer of skin (Kennedy and Wess, 2003). The collagen is made up of specific sequences of amino acid to form polypeptide chains which are woven into three. Three polypeptides chains twist together and form collagen helixes, known as collagen molecules. These molecule bundles would form strands of collagen fibrils which assemble to become collagen fibres (Kennedy and Wess, 2003) (Figure 2.1)

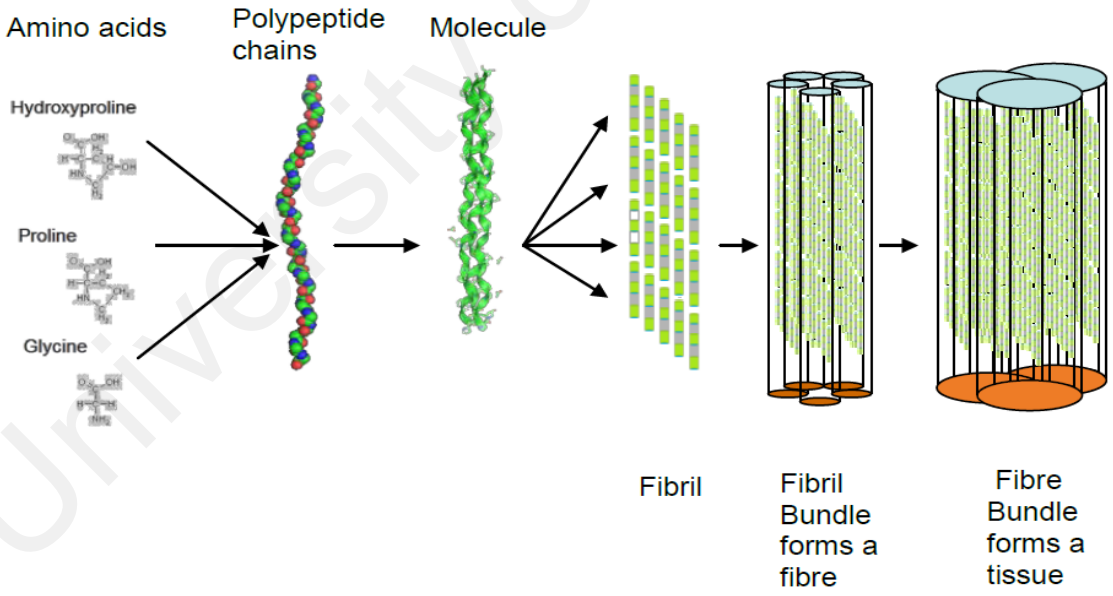

Figure 2.1 The hierarchical structure of collagen. Reproduced from (Kennedy and Wess, 2003)

Due to the distinct hierarchical level of collagen structure, many experiments had been conducted to investigate the relationship between these structures to the mechanical properties of tissue. Previous studies showed that the collagen fibrils are important contributors to the mechanical behaviour of tissue (Cameron et *al*., 2002, Puxkandl et *al*., 2002, Gutsmann et *al*., 2004, Eppell et *al*., 2006, Strasser et al., 2007). The collagen fibrils are formed by self-assembly of collagen molecules. The fibrils have cylindrical shape of diameter in the range of 10 to 500 nm with periodically banded pattern of ~67 nm called D-band (Hulmes et *al*., 1995). These bands can be observed using electron microscopy and atomic force microscopy. Hodge and Petruska first explained about these distinct patterns via the appearance of dark and bright bands in their collagen molecules model called gap region and overlap region respectively (Hodge and Petruska, 1963) (Figure 2.2). The D-band is measured from the length of overlap to gap region.

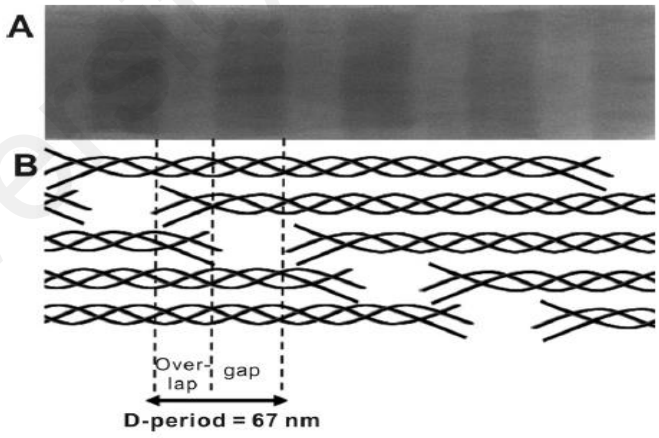

Figure 2.2 The orientation of overlap and gap region that make up a distinct D-banding pattern. Reproduced from (Yang, 2008)

2.2. Mechanical testing on skin tissue

The mechanical properties of skin depend on a few factors. Some studies had been conducted to investigate the influence of age, wrinkles and wetness on skin mechanical behavior (Daly and Odland, 1979, Diridollou et *al*., 2001, Sopher and Gefen, 2011). The study conducted by Daly, (1979) and Diridollou *et al.*, (2001) showed that the elasticity of the skin decreased as the age increased. As previously explained, the collagen contributes to the mechanical properties of skin. In this case, as the age increase, the collagen synthesis decreased, thus decreasing the elasticity of the skin. Besides, Sopher and Gefen, (2011) stated that the shear stresses on the skin increased as the age increase, wrinkle deeper and skin in wet condition.

There are two distinct ways of performing mechanical testing on skin; in vivo and in vitro. The main difference between these two methods is that, the inventor test involved performing the test with the skin excised from the body while testing in vivo is performing the test with the skin still in the body of cadaver or living human.

2.2.1. In Vitro Testing

The in vitro tests were carried out so that the results obtained can be used to inform about important influence on skin function in vivo and basic mechanical properties of skin such as strength and elasticity. In vitro methods involve the removal of skin samples from the body. The skin will be excised from the body, therefore the site and orientation of the specimen are very important, as the resting tension of skin resulted from the structural strain or normal habitual body movements still exist post excision (Edwards and Marks,

1995). Therefore excision care must be exercised to minimize stretching of the sample so that the effects of strain are still obvious many hours after removal of the stretching force. For in vitro experiments, specimens obtained from human are from various body sites like the abdomen, thorax, thigh and volar forearm. In a study done by Christensen *et al*., (1977), the black people skin was chosen because the viable epidermis could better be distinguished from the stratum corneum through the traces of pigment.

Most researches dated conducted in vitro test to measure the tensile properties of skin which is uniaxial tensile test (Wildnauer et *al*., 1971, Daly, 1982, Edsberg et *al.*, 1999, Ní Annaidh et *al*., 2012). This test is the simplest test can be conducted to obtain the basic information of skin mechanical properties. The stress and strain applied can easily control and measured using standard equipment. In tensile test, the sample is cut into a dumbbell shape and the middle part is considered the sample under test while and the larger ends are gripped to a tensile testing machine such as Instron. A strain uniform throughout the sample thickness was considered from this arrangement once the specimen was stretched (Edwards and Marks, 1995).

Daly, (1982) performed uniaxial tensile test of skin excised from fresh cadaver's abdomen. The deformation of skin from the applied stress was plotted and yielded the graph as similar as in Figure 1.3. The result obtained shows the relation between dermal obtained from human abdomen with the non- linear stress strain relationship from tensile test. In addition, he also calculated Young modulus of the dermis in this study by computing a slope at the initial linear part of the curve and found that a strain of below 0.4, the Young modulus was 5 kPa (Daly, 1982).

Edsberg *et al*., (1999) conducted a study to compare the tensile properties of human foreskin when subjected to static and dynamic pressure. The pressure conditions were varied to mimic the behaviour of human heel on various support surfaces. A deformation rate of 31.8 ±1 mm/min was chosen for the uniaxial tensile test of 50 and 170mm Hg static pressure and 110-170 mm Hg dynamic pressure exposed before mechanical testing. The results depicted similar non -linear curve as in Daly. It was found that the skin becomes stiffest when subjected to 50mmHg static pressure while the skin was least stiff when subjected to 170mmHg static pressure. However, for the skin subjected to dynamic pressure, the skin was in intermediate stiffness. Thus, from this study it was concluded that increasing the pressure might lead to less stiffness of the skin. Based from this study, the findings suggested that pressures influenced the mechanical properties of skin. It implies that tissue of skin might fail to resist pressure on it and lead to more serious problem. This study helps to understand the implications of pressure for patient who often suffered from decubitus ulcer.

In the previous review, the authors conducted uniaxial tensile test to measure the viscoelastic behaviour of the skin without considering anisotropic property. In a study done by Ní Annaidh *et al*., (2012) they developed a new experimental method to test the anisotropic characteristic of human skin using uniaxial tensile test. The main focus of this study is to investigate hyper elastic properties of skin and how they vary according to orientation and location with respect to the Langer lines. The skin samples were excised from cadaver's back (male and female) into a dog bone shape specimen with the epidermis and any underlying adipose tissue removed. Besides, the specimens were excised from

various orientations to correlate the specimens with the direction of the Langer lines. The authors grouped the orientation based on parallel, perpendicular and 45^{o} to Langer lines and grouped the location to upper back, middle back and lower back. From the findings, it was found that there was significant effect of the orientation of Langer lines (parallel, perpendicular or at 45◦ to the Langer lines) on the Ultimate Tensile Strength ($P < 0.0001$), the strain energy ($P = 0.0101$), the elastic modulus ($P = 0.0002$), the initial slope ($P = 0.0375$), and the failure stretch ($P = 0.046$). Besides, it was also found that the location of the specimen upper back, middle back and lower back of specimens to have a significant effect on the UTS ($P = 0.0002$), the strain energy ($P = 0.0052$) and the elastic modulus ($P = 0.001$), but neither on the failure stretch nor the initial slope

In paper by Holt *et.al* (2008), they quantified the mechanical behaviour of human skin under low magnitude shear loads over physiological relevant frequencies to mimic the behaviour of skin in vivo. Strain sweep, frequency response, as well as creep and recovery measurements were made on whole human skin and dermis only. The data obtained show that the elastic modulus (G') and viscous modulus (G") increases with frequency of oscillation. Values of G' and G'' were slightly higher for dermis-only samples compared to whole skin. Across this range of frequencies and under these low magnitude shear loads, skin is a complex viscoelastic composite with a rigidly elastic upper epidermal layer and an underlying viscoelastic dermal layer. Furthermore, a time-dependent shear stress of 5 and 10 Pa were applied to whole skin and dermis-only for 300 s at 37 ^{o}C to measure creep. The whole skin biopsies showed an initial elastic response of ~1.74 s for both applied stresses of 5 and 10 Pa. In contrast, the dermis only showed ~2.84 s of the initial elastic response for

both applied stresses. Based on the creep data, the dermis is significantly more compliant than whole skin, thus implying that much of the elastic rigidity is provided by the epidermis. In this study, it showed that whole skin showed strain hardening, while the dermis-only showed stress softening.

Shergold et *al*., (2006) conducted uniaxial compression test on porcine skin to compare with silicone rubber behaviour. The author chose pig skin as the constitutive response of pig skin is close to normal human skin, while silicone rubber of model of B452 and Sil8800 were used as comparison. It was suggested that silicone rubber is a potential model for skin in vitro because of its constitutive response and strain sensitivity is close to human skin. In the study, it was found that the porcine skin strain hardened more rapidly compared to silicone rubber. Besides, the pig skin has greater strain rate sensitivity, thus allowed it to become stiffer and stronger as the strain rate increases. In comparison, the silicone rubber became stiff only when the strain rate exceeded 40/sec.

Munoz et *al*., (2008) characterised male and female mice skin tissue under large deformations using uniaxial test. The large deformations were conducted under monotonic and cyclic loading. The monotonic uniaxial test was done using 15mm/min rate of deformation while cyclic loading was performed by subjecting the specimens to nine ramp cycles with 0.25N increment. The result showed that there was no statistical different between both group at the same loading cycle under monotonic test with maximum strain for male and female of 1.26 ± 0.035 and 1.18 ± 0.083 respectively. However, there were large differences in maximum stress at the same number of loading cycles observed as the

stress was 0.61 ± 0.16 MPa for male while 0.78 ± 0.32 MPa for female group. This study suggested that at large deformation, inelastic strain and stress softening is present in the skin.

Zak et *al*., (2011) investigated mechanical properties of skin obtained from domestic pig foetuses with respect to its structure. The skin samples were excised at different region from the pig; nuchal region, dorsal region, lateral abdominal region, cranial abdominal region, and thoracic limb region. The samples were deformed at a rate of 5 mm/min until they ruptured. From the non-linear stress-strain curves obtained from the experiment, it was shown that thoracic limb region uniaxial test produced highest elasticity with 7.68 ± 3.96 MPa while skin collected from cranial abdominal region displayed lowest value of Young's modulus with 4.02 ± 3.81 MPa. Therefore the study concluded that the changes of mechanical properties are attributed to the specific arrangement of collagen fibres in the skin are varied in difference site of excised skin.

2.2.2. In Vivo Testing

In vivo mechanical testing is conducted to the skin directly on the body. However, only the top layer of skin is accessible for mechanical testing. Thus, the mechanical properties of the skin are investigated from the whole skin; therefore the influences of different skin layers are difficult to be distinguished.

Barbenel and Evans, (1977) conducted experiments to study the time dependent of human skin by applying a deformational torque on the skin. In this experiment, they used a system consist of servomotor to produce constant rate of deformation with a strain gauge

attached at the motor shaft and a detachable disk would be stuck to the skin to measure the torque. The mechanical input of the rotation was held constant at certain period, and the torque was recorded. The result obtained from this experiment shows nonlinear deformation where in the initial deformation, a low amount of torque was produced; however as the deformation rose, the torque increased until stiffer or linearly range was reached. The viscoelastic behaviour of the skin was observed from the decreased of torque even constant displacement was applied. In this paper, they continued their investigation by applying sinusoidal displacement to the skin to study the viscoelastic property. As a result, the nonlinear behaviour was also observed. It was revealed that small amplitude of displacement, the torque was linear, and as large deformation was applied, the nonlinear phase entered.

An interesting study was done by Cooper *et al*., (1985) to investigate the comparison of mechanical properties between normal, dry and glycerol treated skin. In this study, they measured the viscoelastic property of different types of skin by using gas bearing electrodynamometer (GBE). Prior to measurement by GBE, the subjects were required to apply 0.6ml of 40% glycerol solution to the outer calf and the same amount of water was applied at the other calf. This treatment was done twice daily for three days. During GBE measurement, an oscillating force was applied to the skin thus resulting in strain. The data recorded was then analysed further to obtain the elastic modulus (E') and viscous modulus (E''). The study showed that the elastic modulus increasing as the skin grades increased, hence showing that the skin is stiffer as the skin condition is not good. In addition, they

suggest that glycerol helps to soften skin more significantly by lowering the elastic modulus as compared to water.

Boyer *et al*., (2012) performed a non-contact in vivo method to measure the mechanical properties of human skin. The test was investigated to compare the Young Modulus between 2 groups; group 1 which is consisted of 14 healthy young women aged 23 to 25 years old while group 2 which is consisted of 14 healthy old women aged 60 to 63 years old. The area of interest in this research was volar forearm at 60mm from the elbow. In order to perform the non- contact experiment, Boyer and his team developed a device based on air flow system to exert force on the skin, and a high speed triangulation measurement as shown. This developed device avoids the use of adhesive tape to bond the probe to the skin which might cause measurement error (Fujimura et *al.,* 2008, Fleury et *al*., 2010). The controlled air flow system will produce pressure to exert on the skin, while the laser sensor will measure the gap between the output pipe and the skin. In the experiment, the forces applied on the skin were 10, 20, 30, 40, 50 and 60mN and held at 2s and 7s. Based from the results obtained, several parameters were calculated to obtain creep (cr) and the reduced Young modulus (E*) of the skin. The creep properties of skin showing that the creep increases with load for both group, and the creep remain constant as the load increases from 40 to 60mN. The Young modulus obtained from this in vivo method showed that the modulus for young people was in the range of 13 to 14.5 kPa which is higher compared to old people which was in the range of 6 to 8kPa.

Pailler-Mattei and Zahouani, (2004) performed an indentation test with small load on the internal forearm by studying the adhesion forces between the indenter and the skin. This study was done to investigate the effect of surface lipidic film on skin behaviour for normal skin and dry skin. There were 10 young women aged 30 years old involved in this study. The indentation device is controlled by displacement. This device will continuously measuring the induced force as a function of penetration into the material. The result showed that as the applied load increases, the penetration increases for both normal and dry skin and it was shown that at the early stage of penetration, the effect of adhesion force between indenter and skin due to the presence of thin liquid film on the skin was observed. In this experiment, the normal skin test later was manipulated by varying the indenter load and indentation speeds. The adhesion forces were recorded at speed of 500μm/s with varying loads of 20, 30, 40, 50 and 80mN and at fixed load of 50mN with varying speeds of 300, 500, 700 and 900 μm/s. The result concluded that the percentages of deformation of normal skin were increased when load increased. Besides, as the indenter speed increased, the deformation slightly decreased due to the increases of adhesion forces.

The constitutive model is used to describe the physical properties of a material. Several authors used constitutive model to simulate the mechanical properties of skin in vivo (Diridollou et *al*., 2000, Khatyr et *al.*, 2006, Pailler-Mattei et *al*., 2008, Zahouani et *al*., 2009). However, these experiments were conducted by assuming that the skin is linear and isotropic. Flynn *et al*., (2011) introduced an experiment to investigate the nonlinear, anisotropic and viscoelastic properties of human skin from different areas of arm by using a force sensitive micro robot and finite element analysis. The tests were performed on

posterior upper arm, upper anterior arm, and lower anterior forearm. The force on the micro robot was induced when a probe attached to an actuator resulting in cyclical deformation of skin. The deformations were manipulated by displacing the probe at 0, 30, 60, 90, 120 and 150^{o}. Finite element analysis (FEA) model of the experiment set up and mathematical constitutive model were constructed for analysis to compare with the experimental results. From the result, it was shown that anterior upper forearm was the stiffest while anterior lower forearm was the least stiff.

Recently, Bismuth et al., (2014) studied the biomechanical properties of dog skin by uniaxial extension. The tensile test machine was custom-built and performed on the non-isolated skin first before applying the same test on excised skin. The study showed that Rigidity was low at low strain, however as the strain increased at 20%, the Rigidity was dramatically increased. The study demonstrated that the extension set up as in their experiment can be employed as 'true in vivo' mapping tool in order to determine the biomechanical properties of skin during wound healing or for characterization of human skin disease when the dog as the animal model.

2.3. Biomechanical properties of expanded skin

The biomechanical properties of expanded skin are not many reported. In the late 80's Schneider et *al*., (1988) conducted the first ever reported study on biomechanical properties of expanded skin. The albino guinea pig skins were expanded sequentially every 4 days using Radovan type tissue expander. The expander was left for 4 days once maximum volume was achieved prior to explantation. Tensile test was performed on the expanded

skin excised from peripheral and centrally expanded samples. Based from the results, it was concluded that the expanded skin strength was reduced by 35% compared to non-expanded skin. It was shown that the strength coefficient of centrally expanded skin specimen was 9.15 in.lb/in^3 compared to control with 30.11 in.lb/in^3. Meanwhile, the maximum stiffness reported from the study showed that the expanded skin featured 4.56 lb/mm^2 while normal skin demonstrated 12.98 lb/mm^2. The study showed that there was no significant difference for skin excised from peripheral margin for both.

Timengga et *al*., (1990) conducted tensile test on expanded skin obtained from rabbit skin. Silastic balloon were implanted in the dermis at the dorsal thoracic area of the animal and inflated on a daily basis for 10 days. In separate animals, the balloon was implanted at the same area without inflating the balloon and served as sham-operated control group. The harvested skin was tested to failure with a crosshead speed 6.35 mm/min. The study found that the maximum stiffness of the expanded skin was reduced to 60% while 35% for sham operated group as compared to normal skin, thus suggesting that the expanded skin was less stiff compared to non-expanded skin. In histological experiment, dermis layer of expanded and sham-operated skin was thickened and loosely packed collagen bundle with increased diameter was observed.

In a study by Zeng et *al*., (2004), the samples taken from dog's skin. The experiment was done by varying the expansion regime and comparing its biomechanical properties with normal and sham- operated skin. One group of the skin was expanded using rapid expansion every other day for two weeks, while the other was expanded weekly for two

compared to normal free graft. The study demonstrated that the biomechanical characteristic of expanded free graft is close to normal skin.

2.4. Atomic Force Microscopy

The invention of AFM enables researchers to view surface topography of biological sample at ultrastructural level in high resolution by investigating the interaction forces between a sharp tip and sample surface. The topography is imaged by scanning parallel lines on the surface of a sample with a sharp tip fixed at the end of a cantilever in rectangular pattern. During raster-scanning, the cantilever deflects and the deflections causes laser light shined through the tip to be deflected as well. A sensitive photodiode will detect the reflected laser light to construct the sample's surface topography. The system combination is illustrated as in Figure 2.4.

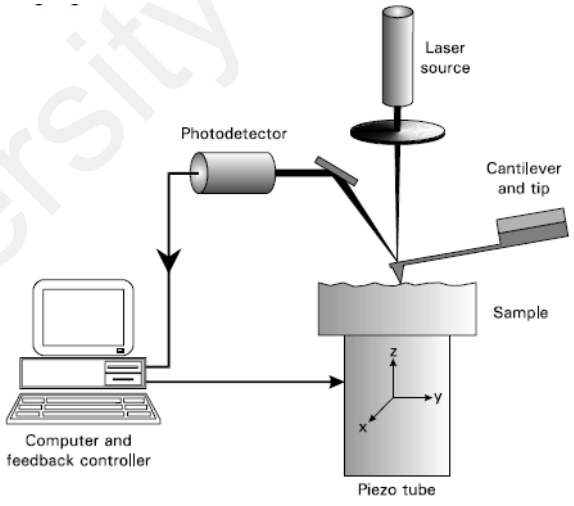

Figure 2.4 The illustration schematic representation of AFM components. Reproduced from (Leite et *al.*, 2007)

For imaging, the AFM can work in two modes; contact mode and non-contact mode. Contact mode is the first imaging mode developed and most widely used. As the name suggest, contact mode required the tip to directly touch the surface in constant force or constant height. If the constant force is applied, the feedback loop will keep the cantilever deflection constant; however if the constant height is employed, the cantilever is held at the same height throughout the scanning with the feedback off (Kasas et *al*., 1997)). Because of the constant touching of the tip on the surface, the main advantage of this mode is its height sensitivity in z-axis. On the other hand, the disadvantage of contact mode is the tendency of broken tip and sample damage as the applied force is increased. Non-contact mode utilized oscillation of cantilever at certain frequency to a distance above the sample's surface. Attractive forces induce changes in amplitude, phase and frequency of the lever, and are used by the AFM to keep the tip sample distance constant (Leite et *al*., 2007). The cantilever used in this mode is basically much stiffer compared to contact mode's in order to prevent the tip from snapping on the sample due to attractive force. As the tip is not directly touching the sample, the main advantage of non-contact mode is it allows for imaging of very soft biological sample. Besides, the force applied in non-contact mode is lower compared to contact mode, thus limiting the signal detection., Due to this reason together with large tip sample distance, the image produced using this mode is in lower resolution.

In recent years, the AFM has been upgraded to be able to determine the mechanical properties of nano-scale size biological sample (Strasser et *al*., 2007, Wenger et *al*., 2007, Graham et *al*., 2010, Janko et *al*., 2010, Shen et *al*., 2011). The AFM tip able to probe an

extremely small area and permits high sensitivity to small forces. Therefore aside from high resolution imaging, AFM also is a powerful tool to investigate mechanical characteristics of small size specimens down to single molecule. Force spectroscopy is one of the modes available in AFM to conduct mechanical testing. Force spectroscopy is performed once the imaging has been stopped by approaching and retracting the cantilever tip from the sample while the interaction between the tip and sample (cantilever deflection) is measured. The reading is illustrated in a force-distance curve (Figure 2.5) which contains information about the force interaction between tip and sample surface as a function of relative tip-sample distance. Upon approaching, as the tip moving to the sample, the cantilever remains undisturbed until the tip bend down toward the sample due to attractive forces. The tip keeps bending until repulsive forces generated by the electron between tip apex and sample balances the attractive forces. This point marks as a contact point from the force distance curve. If the piezo continues to push the tip towards the sample, the cantilever will deflect upwards. The extend of the deflection depends on stiffness of a sample, and the result is reflected on the force distance curve produced by force spectroscopy. Based from the force distance curve, linear and steeper slope after contact point indicates stiffer materials. During cantilever retraction, similar force distance curves are produced as the tip is pulled away from the surface. However, as the cantilever retracted, the tip remains in contact with the surface sample due to adhesion forces, thus causing the cantilever to be deflected downwards. At some tip-sample distance, the force from the cantilever overcome the adhesion forces and frees the tip. If the surface is hydrophilic, the water layer on the surface

might attracted to the tip and form strong adhesion forces when the cantilever retracted from the surface.

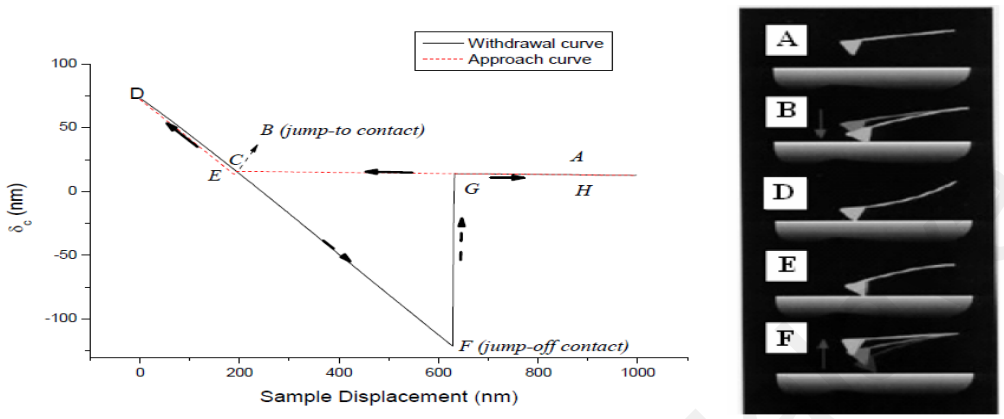

Figure 2.5 The force diagram obtained from approaching and retracting tip from sample surface. A-The tip is approaching to sample without deflection of cantilever. B-Due to the attractive forces between tip and sample, the tip jump to contact with the sample and produced snap in (C). Due to the continuous downward movement of piezo, the tip continues to touch the surface and deflected the cantilever upwards. The deflection of the cantilever is recorded as force in D. Once the motion of the tip is inverted, the cantilever retracts and follow path E. Depending on the adhesion forces between the tip and sample, the tip is released at different jump off contact (F) moment. Once the adhesion is overcome, the tip jumps to its normal position G and continues to retract without being disturbed by the sample. Reproduced from (Leite et *al*., 2007)

2.5. Collagen Fibrils structure and Mechanical Properties by AFM

Numerous studies have been done on surface topographical using AFM technology of biological sample of various sizes from cell to smaller structures. However a restriction is arises when tissue sample is concern owing to accessible z-range of tip is limited to 15 μm maximum, thus prohibiting the observation of extremely rough structures (Kasas et *al*. 1997). Therefore, some authors used biological ultrathin sections and exposed to fixation and embedding procedures prior to AFM imaging (Matsko and Mueller, 2004, Li et *al*., 2008).

Graham et *al*., (2010) used tissue freezing and cryo-sectioning method to prepare 5μm tissue thin section sample. The study scanned structures of collagen fibrils in skin, cartilage, invertebral disc and elastic fibres in aorta and lung in situ working in non-contact mode. From the findings, it was revealed that the collagen fibrils in the skin is arranged in basket-weave like structure and the ~ 67nm distinct banding pattern of collagen fibrils in the tissues was clearly observed. In addition, this study concludes that the use of cryosectioning and non-contact AFM imaging permit manipulation of biological sample without interfering its structural integrity. Furthermore, the same region on the tissue may be repeatedly imaged.

Prior to the advent of AFM as imaging tool, the structural and mechanical properties of collagen fibrils was studied using X-ray diffraction (Mosler et *al*., 1985, Fratzl et *al*., 1998, Wilkinson and Hukins 1999, Cameron et *al*., 2002, Puxkandl et *al.*, 2002). Among the authors, Mosler et *al*., (1985) conducted series of experiments to study the fibrils elongation during mechanical strain. The collagen fibrils obtained from rat tail tendon was strained and its elongation was monitored using time resolved X-ray measurement. The D-banding of the stretched fibrils increased to 67.6 nm from 67nm due to stretching of collagen molecule. The study suggests that the sliding of collagen molecule helps to further increase the D-band.

Wenger et *al*., (2007) conducted AFM nanoindentation to determine the Young's Modulus of single type I collagen fibrils of rat tail tendon. The dissected collagen fibrils were fixed using phosphate buffer saline at 4^{o}C before imaging. The elastic modulus

obtained from nanoindentation at the overlap region of tendon collagen fibrils was ranging from 5 to 11.5 GPa. This study made an interesting finding which suggests that the fibrils are made of subfibrils which aligned along the fibrils axis.

Graham et *al*., (2004) investigated the biomechanical properties of single collagen fibrils cultured from human fibroblast. Using AFM force spectroscopy, the fibril was stretched to an extension of several microns. The stretching of the fibrils was accomplished by adsorbing the tip to the sample and stretches the fibrils gradually (Figure 2.3). From the stress-strain curve, it showed that above 4% strain, the young Modulus was 32 MPa (Fig 2.4). The study suggest discontinuity happened at 1.5 to 4 nN force was due to structural reorganization of collagen monomers

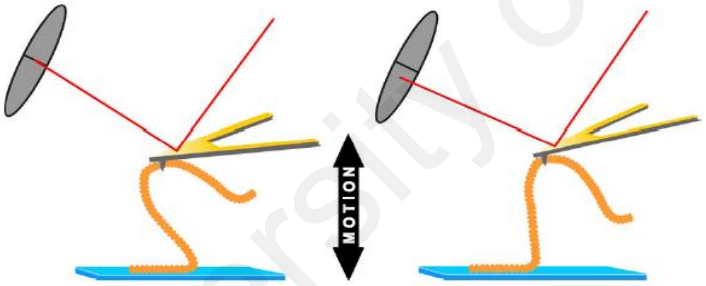

Figure 2.6 The illustration of force spectroscopy on collagen fibrils (Reproduced from (Graham et *al*., 2004)

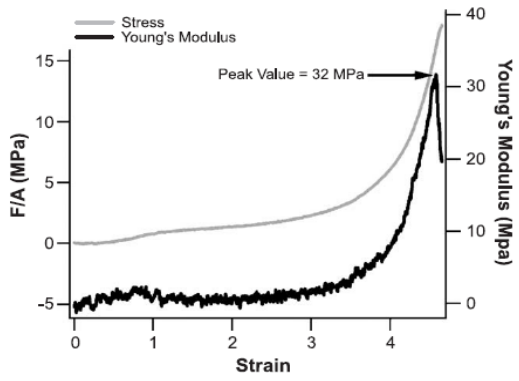

Figure 2.7 The stress-strain curve obtained from force spectroscopy of single collagen fibrils (Reproduced from (Graham et al., 2004)

Eppel et *al*., (2006) studied the elastic properties of collagenous tissue using microelectromechanical system technology. The technology was developed to perform large strain uniaxial test on collagen fibrils isolated from sea cucumber's dermis and conducted cyclical loading prior. It was found that the elastic modulus reduced from 930 MPa with repeated cyclic loading. However, there was no significant difference of moduli at 10 and 100 Hz loading frequency. Years later, the team utilized the same technology to study the viscoelastic behaviour of the tissue (Shen et *al*., 2011). The elastic modulus found was 123 MPa with fast time response and slow time response fitted from Maxwell-Weichert model were 7 seconds and 102 seconds respectively.

Strasser et *al*., (2007) performed nanoindentation to investigate the elastic properties of the outer shell and inner core of single collagen fibrils. The individual collage fibrils were cultured from collagen solution prepared from calf's skin. Aside from imaging, the authors utilized AFM as a microdissection tool to expose the inner core of the collagen fibrils.

From nanoindentation force spectroscopy conducted on both structures, it was found that there were no major differences of banding pattern on the outer shell and inner core of single collagen fibrils. Besides, the study suggested that the elastic properties of both structures were comparable with average of 1.2GPa. Meanwhile, the adhesion force produced by the inner core was higher compared to outer shell of collagen fibrils.

A study conducted by Yang et *al*., (2008) manipulating AFM to perform bending test on native and carbodiimide -cross-linked single collagen fibrils. The bending test was done by moving a tipless cantilever along single fibrils in z-direction. The output signal from fast scanning direction was used to drive piezo movement while the slow scanning direction was used to move the cantilever along the fibril. From the micromechanical testing, it was found that the bending modulus of native and cross-linked single collagen fibrils has no significant difference with 1.0 – 3.9 GPa and 1.7 – 3.1 GPa respectively in ambient condition.

Chapter 3. METHODOLOGY

3.1. Animal Preparation

The animal ethical approval was obtained from Institutional Animal Care and Use Committee (IACUC) of the Faculty of Veterinary Medicine, University Putra Malaysia. Adult male Dopper sheep of age 2 years and average weight of 40kg were used in this study. Four animals each of control and expanded skin group were used. All procedures were performed under general anaesthesia using a cuffed endotracheal tube fasted prior to the surgery. The sheep were injected with ketamine 10% (Pharmaniaga, Malaysia) and maintained with isoflurane concentration set at 5% where depth of anaesthesia was monitored and adjusted accordingly.

The surgical field was thoroughly washed with 0.015% chlorhexidine gluconate and 0.15% cetrimide solution. A subcutaneous pocket was created by blunt dissection in a tension-free manner. A gamma sterilized anisotropic self-inflating tissue expander of 20 mm diameter and 3 mm thickness made by OXTEX was slid through and implanted within the preformed pocket in the dorsolateral region of the lower limb (Figure 3.1). The surgical wound was sutured with interrupted 5-0 vicryl (Ethicon Inc, Johnson & Johnson, UK). In addition, three sutures were tied posterior to the expander to prevent device displacement and to close dead space. The animals were formally assessed on a daily basis. Photos of expanded skin and x-rays were taken and shown as in Figure 3.2 a,b.

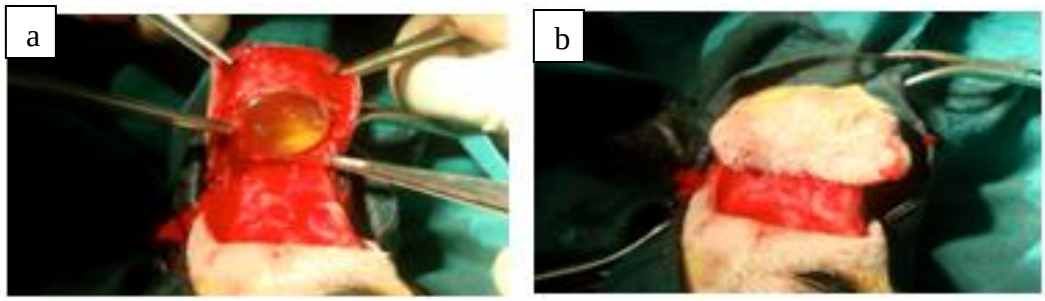

Figure 3.3 a) The deflected skin tissue b) the explanted skin

3.2. Surface Topography

3.2.1. Sample preparation

The specimens were cut into smaller pieces and the cross section of each piece was embedded in Optimum Cutting Temperature (OCT) compound (Thermo Fisher) and kept inside the Cryostat freezer at -14^{o}C until it frozen. All frozen specimens were cryo-sectioned to a thickness of 50 µm (Wen et *al*., 2012) using Cryostat (Leica), mounted on glass slide and dried at ambient temperature to ensure that the specimen section is adsorbed to the glass properly. The glass slides were then rinsed with distilled water to remove excess compound and left to dry again at ambient temperature (Graham et *al*., 2010).

3.2.2. 3D Optical analyser

The average surface roughness in selected area of expanded and normal specimens was measured using the 3D Optical analyser (Alicona, Germany). Prior to data recording, pilot studies had been done to select the best magnification to view the surface. Based from the studies, it was shown that magnification of 20X was best suited to be used, as higher

magnification resulted in blurred images. This testing is also useful in order to determine the suitable tip for use in the AFM imaging.

3.2.3. AFM Imaging

The AFM images were obtained using NanoWizard® 3 AFM (JPK Instrument, Germany) using contact mode in air. A gold coated silicon nitride cantilever of resonant frequency of 66 kHz and 0.284 N/m nominal spring constant (HYDRA6R-100NG, AppNano) was employed in the imaging. The sharp tip of radius of 0.01 nm allows for high resolution imaging and force constant of 10 nN (Jastrzebska et *al*., 2005) was applied during imaging. Two channel windows were observed during imaging. The two channels are the height channel which corresponds to the topography of the sample and the error signal channel for direct observation of the collagen fibrils. The maximum scanning area in X and Y directions are both 10 μm x 10 μm and the maximum height (z-range) is 15 μm. The time taken to complete one frame of 512 x 512 pixels was about 300 s.

3.3. Biomechanical Testing

3.3.1. AFM Force Spectroscopy

Force spectroscopy was performed on the collagen fibrils identified from the topographic scan by generating 10 points on the centre region along a single collagen fibril with (Janko et *al*., 2010). The force curves were recorded for each point to measure the elastic modulus. The elasticity was measured from fitting the contact region of the force curve using Hertzian model (JPK Instrument). The Hertz model approximates the sample as

an isotropic and linear elastic solid (Strasser et *al*., 2007). Besides, it is assumed that the indenter is not deformable and there are no additional interactions between sample and tip. The cantilever obeys Hooke's Law, F = k x where F is the force exerted on the sample, k is the spring constant of the cantilever and x is its deflection. Considering the use of 0.01 nm paraboloid tip (as advised by the JPK Instrument scientist) in this experiment, the Elastic modulus for each curve was calculated using (Strasser et *al*., 2007)

$$z = \left[\frac{3.k.(d-d_0).(1-\nu^2)}{4.E.\sqrt{R}}\right]^{2/3} + (d - d_0) + z_0 \quad (3.1)$$

Where d_0 and z_0 are the corresponding values of the cantilever deflection and the z-piezo extension at the contact point, E is the Young modulus, v is the poisson ratio (0.5) and R is the tip radius. All images and force spectroscopy data were processed using JPKSPM Data Processing software. The images were filtered to generate better images while the force spectroscopy data were processed to calculate average elastic modulus.

3.3.2. Tensile test

For the uniaxial tensile test, the skins were cut to 5 x 20 mm diameter with the average thickness of 1.3 ±0.5 mm for normal skin while 2.0 ±0.5 mm for expanded skin with parallel with the body as in Figure 3.4 . Load is applied to the specimen at a constant rate of 10 mm/min (Zhang et *al*., 2006) using Instron (MicroTester) with 2 kN load cell and force-elongation curves was obtained. During mechanical loading, 5 x 4 mm of the end sample was gripped by the clamper and the test length was 7 ± 0.5 mm.

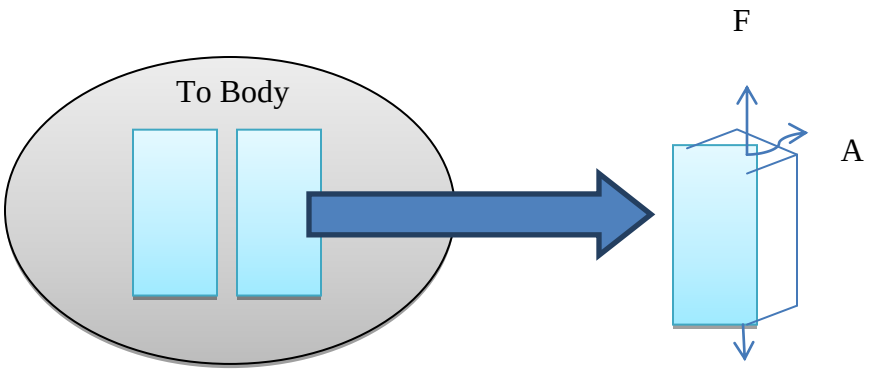

Figure 3.4 The harvested skin and its orientation during tensile test

The stress-strain curve was then generated and initial elastic (E_0) and terminal moduli (E_∞) were calculated at the initial slope and the linear region of the curve respectively (Figure 3.5). Before the proper test, all samples were subjected to few loading-unloading cycles for preconditioning of skin tissue (Zhang et *al*., 2006, Liu and Yeung, 2008, Munoz et *al*., 2008, ŻAK et al., 2011). In this experiment, it was noticed that the stress-strain curve become stable after third cycle, therefore the specimens were regarded as preconditioned and data in the fourth cycle were used for analysis. The stress-strain curve was then generated by using (Zeng et *al*., 2004, Zhang et *al*., 2006)

$$Stretch\ ratio, \lambda = \frac{L}{L_0} \quad \text{with} \quad \Delta L = L + L_0 \tag{3.2}$$

where L is the length of the extended sample, L_0 is the gauge length and ΔL is the extension of sample.

$$Eulerian\ Stress, \sigma = \frac{F}{A}\ \lambda \tag{3.3}$$

Where F is the exerted force and A is the surface area of the specimen. The Green strain was calculated from

$$Green\ Strain, \varepsilon = \frac{1}{2}(\lambda^2 - 1) \quad (3.4)$$

Thus, from (3.3) and (3.4), the Elastic modulus was calculated from the slope of the curve from

$$Elastic\ Modulus, E = \frac{\sigma}{\varepsilon} \quad (3.5)$$

Besides, limit strain was calculated for both groups by extending the slope at linear region until intercept at the x-axis. Limit strain is the extension produced at maximum stress until the sample fail.

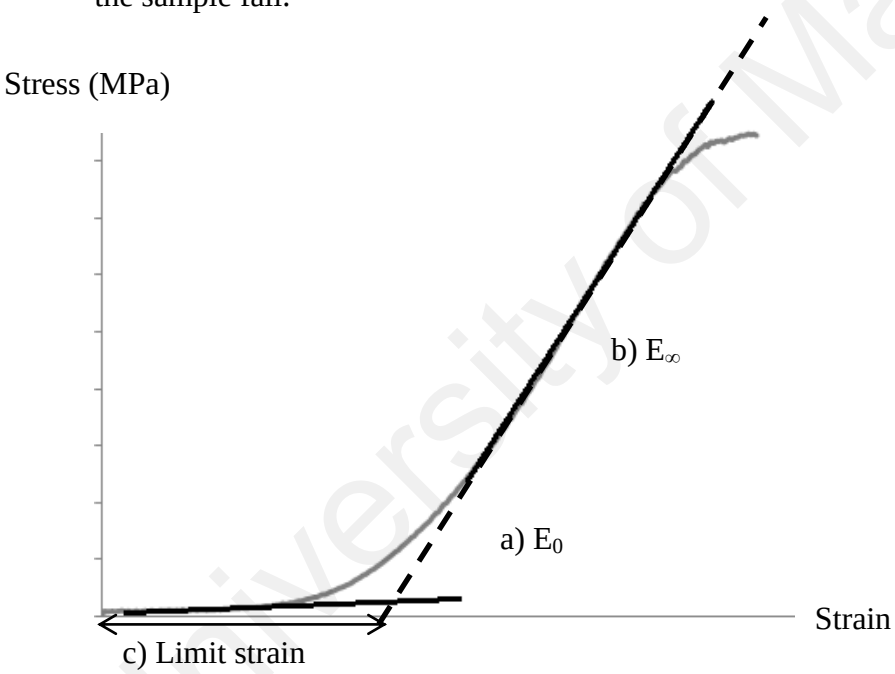

Figure 3.5 The tensiometric parameters. The elastic moduli of (a) E_0 and (b)E_∞ are calculated from the slope of initial region and linear region respectively. The limit strain (c) is calculated from interception point of linear region slope on the x-axis.

3.3.3. Statistical analysis

All datasets were analysed using the independent two sample Student's t-test. Differences are considered to have statistically significant if $p < 0.05$ with confidence level of 0.05. The statistical analysis was processed using SPSS 16.0 and Microsoft Excel 2010.

Based from the figures and statistical analysis, it was shown that the expanded skin has significantly lower height ($p=0.005$ & $p = 0.02$) and surface roughness ($p =0.021$). The investigation of surface roughness of each sample is also useful as a verification analysis in order to ensure that the surface topography of the samples is able to be mapped by the chosen AFM cantilever. This is because, once the roughness and the height of the samples were known, it is easier to conclude whether the spring constant is stiff enough to be used on the sample. The statistical analysis done using SPSS for z-height, Sa and Ra are shown in APENDIX A, APENDIX B, and APENDIX C respectively.

Table 4.1 The height and roughness of control and expanded skin measured by 3D optical surface analyser.

	Control	Expanded
z- height (µm)	28.70 ± 6.02	14.36 ± 5.19
Sa (µm)	6.33 ± 1.17	3.16 ± 1.63
Ra (µm)	1.42 ± 0.64	0.55 ± 0.27

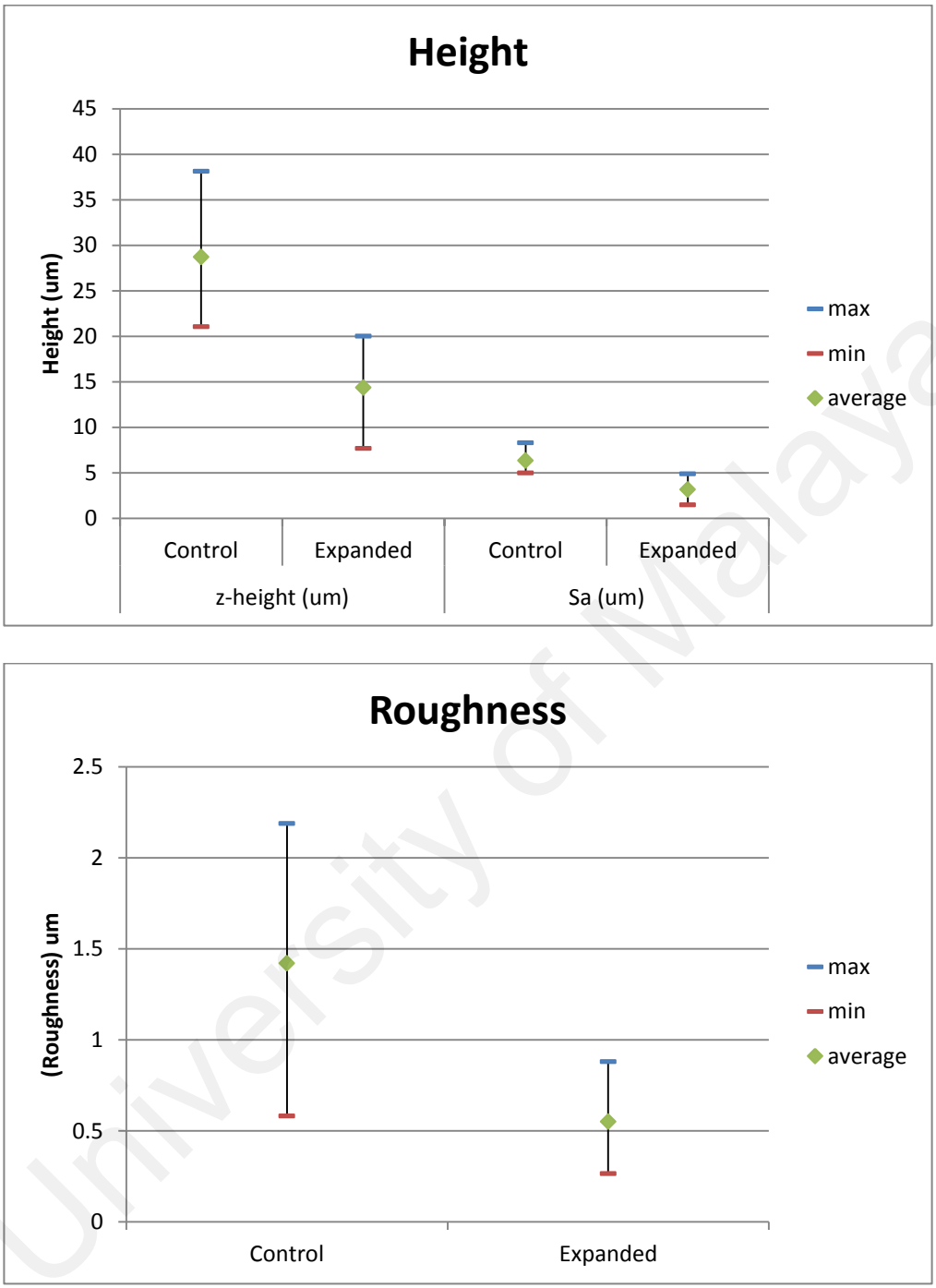

Figure 4.4 The graph of Top: height in a line and selected surface area. Bottom: roughness from one line. The graphs showed that the cross-section surface of expanded skin has significantly lower height differences and roughness compared to normal skin sample.

4.1.2. AFM Images

The collagen fibrils identified from the AFM images were observed to be stacked in basket-weave like structure for both groups of samples. In addition, it was observed that networks of collagen were overlapping with each other. Based from Figure 4.4a, control skin was composed of densely packed collagen. It is expected that the collagen fibres is convoluted in crimp pattern; however such scenario is not clearly observed from the image, due to the fact that the scanned region was randomly selected at only few micrometer scale. Besides, utilizing tissue section for AFM imaging, enable observation of ultrastructural at higher resolution. The topography can be repeatedly imaged at the same region with smaller scale to observe more details structures. It was observed at higher magnification, the banding pattern was clearly revealed (Fig 4.4b).

From the qualitative and quantitative data, it was evidence that the implanted tissue expander had stretched the skin and extended the collagen fibrils. It is believed that the stretched fibrils are due to viscoelastic characteristic of collagen fibrils (Mosler et *al*., 1985, Graham et *al*., 2010, Shen et *al*., 2011). The authors suggest that, when stress is applied to the fibrils, the rearrangement of structural collagen fibrils could happened due to three different ways; the straightening of collagen molecules itself, sliding of collagen molecules from each other or the water molecules expelled from the fibrils and resulting of reorganization of water network.

However, as comparable D-banding value between both groups of experiments, the elongation of the collagen fibrils cannot be proven in this study. This is probably due to two factors; 1) measurement error and 2) tissue behaviour that changes over time. The first factor is considered because owing to the fact that the measurement was done using tool in the software combined with limited view of D-banding sequence. The measurement could be calculated with slight error. Besides, there was no repeatability test done to ensure that the data is reliable. However this factor may contribute to small percentage of the findings because the measurement was done on more than 70 visible distinct banding. Whereas for the second factor, we speculate that it was due to the nature of skin growth. Since the skin behaviour is time dependent, there is high chance that in the long course of expansion, the skin 'components' start to settle down and recover, resembling to that of normal skin (Zhang et *al*., 2006).

4.2. Biomechanical properties

4.2.1. AFM Force Spectroscopy

More than 60 curves were generated for force spectroscopy of control and expanded skin. The displayed curve (Figure 4.8) represents several experiments each for control and expanded skin tissue. The indentation experiments were performed on several random collagen fibrils on the overlap region only. Janko et *al*., (2010) revealed that at the centre of overlap region, the surface is elevated. The force-distance curve derived from expanded skin featured steeper slope as compared to control skin. The average Young's moduli for each sample groups were calculated from individual force curves. The measurement showed that the average of Young's modulus for control collagen specimens was 36.1 ± 29.5 MPa, while the elasticity for expanded fibrils was 45.9 ± 24 MPa. However, statistically, the difference between the average elastic modulus for both group was not significant ($p = 0.064$). The statistical analysis done using SPSS is shown in APPENDIX F.

collagen molecules that lead to the extension fibrils in the expanded skin. A study by Janko et *al*., 2010 proved that changes in molecular structure of collagen contribute to changes in elastic properties of skin collagen fibrils.

It is suspected that the large variation between the two groups is due to different collagen fibrils that lead to different mechanical behaviour, and the uncertainties of fibrils indentation points. This is because some point might be generated on the gap region of fibrils due to unclear image. It was known that the elastic properties of overlap region and gap region are significantly difference (Minary-Jolandan and Yu 2009). According to the authors, elasticity of gap region is almost 100% lower than the overlap region. Therefore a bias toward large fibrils occurred because only those large fibrils were visible in the AFM camera and selected for testing. Thus, the fibrils tested in this study cannot be representative of fibrils population in the sample. (Svensson et al., 2012) suggested that large diameter fibrils produced higher modulus. Moreover, the underlying hard substrates could influence the results of indentation performed on thin sample (Strasser et *al*., 2007).

was shown that the expanded skin tissue displayed higher modulus compared to normal skin. The limit strain of expanded skin was lower compared to control.

Table 4.2 The initial modulus (E_0), terminal modulus (E_∞) and limit strain obtained from uniaxial tensile test

	Control (n=5)	Expanded (n=5)
E_0 (Mpa)	0.27 ± 0.19	0.85 ± 0.67
E_∞ (Mpa)	2.14 ± 1.46	4.4 ± 1.97
Limit strain	0.5 ± 0.16	0.3 ± 0.20

From the statistical analysis, no significance difference between for E_0 ($p = 0.128$) and E_∞ ($p = 0.068$) respectively were observed for both groups. The statistical analysis done using SPSS for E_0 and E_∞ are shown in APPENDIX G and APPENDIX H respectively.

This observation was different with finding in literature probably due to the method of expansion, where the literatures employed conventional tissue expander method in which the skin was expanded by force compared to the self-inflating tissue expander method used in this study where the skin was expanded in physiological condition. On the other hand, this finding correspond to Zeng et al., (2010) and Zhang et al., (2006) which suggested that the expanded skin behaviour would recover and close to non-expanded skin as the maintaining period is extended. Besides, previous studies showed that the mechanical testing was done on the expanded skin with the capsule and panniculus carnosus were removed prior to testing. However Schneider et al., (1988) was criticised by doing so because they eliminated their clinical significance. In the present study, the expanded skin

including the panniculus carnolus and capsule were tested. Therefore, this step might probably affect the significant of the sample modulus.

4.2.3. The stiffening of expanded skin

The results obtained from mechanical testing of collagen fibrils and skin tissue showed that the slight increase of elastic modulus for expanded skin sample. Based from the surface topography and testing, present study demonstrated that expansion of skin cause the collagen fibrils to be stiffened.

Initially, in biological equilibrium, the skin is in a state of bi tension (Pamplona et *al*., 2014). Besides, the collagen fibrils are arranged in dense and crimp pattern. However, as tissue expander gradually inflated and stretched the skin, the fibrils started to rearrange themselves parallel with each other in order to resist the deformation. As the collagen fibrils extended and become straighter, the resting tension increased, and results in it become stiffer (Pamplona et *al.*, 2014). Therefore, once subjected to further stretching i.e. uniaxial tensile test, the relatively straight and stiff collagen fibrils will continue to overcome the load, therefore produce higher elastic modulus. This occasion can be perceived from the limit strain obtained in present study. The limit strain of expanded skin is lower compared to control skin, which is in agreement to the fact that as the collagen fibrils extend and thin, low strain is needed for the fibres to fail once subjected to stress.

Tissue expansion is based on the viscoelastic properties of skin to increase surface area in response to intrinsic and extrinsic forces (Bascom and Wax, 2002). Several studies have suggested that the increase of surface area following tissue expansion resulted from new

tissue being generated by the event called mechanical creep (Squier 1980, Austad et *al*., 1982, Ersek and Vazquez-Salisbury 1994). Besides, in a review reported by Wilhelmi et al., (1998) explained that elongation of skin beyond its inherent extension results in mechanical creep. This mechanical characteristic is a trigger to wound closure techniques such as pre-suturing. However, the author suggested that tissue expansion is the consequences of biological creep with generation of new tissue secondary to persistent chronic stretching force. Although, it is upsetting that the mechanical study in this experiment fail to give any significant clue on the evidence of tissue grow, however, as the aim of this study is to investigate the quality of the expanded skin, this experiment successfully reveal the potential of self-inflating tissue expander to produce new skin tissue with comparable elastic properties to the original tissue. In this study it was revealed from the surface topography that no defibrillation occurs, suggesting that even though the expansion occurred continuously over long period of time, fibres failure does not happen.

4.2.4. Comparison with literature

The Elastic moduli of collagen fibrils obtained in this study are not in reasonable agreement with most literatures probably due to three factors:

1) Method of force spectroscopy
2) Origin of collagen fibrils
3) Fixation of tissue

In this study, we employed the nanoindentation method to determine the elastic property of the sample. The elastic properties represented from nanoindentation test are calculated from

the force applied by the tip-sample system and the resulting deformation of the sample while previous studies on one dimensional tensile stiffness(Graham et *al*., 2004) and bending test (Yang et *al*., 2008) along the fibrils axis. As for the second factor, this study performed the force spectroscopy on the collagen fibrils visible from the skin tissue section. As compared to previous authors, they used isolated or cultured collagen fibrils obtained from sea cucumber (Eppell et *al*., 2006), calf skin (Strasser et *al*., 2007), tendon (Minary-Jolandan and Yu 2009), human skin (Graham et *al*., 2004) and performed the test on individual collagen fibrils. In the present study, difficulty arises during the recognition of fibrils because some fibrils are easily identified while others have more complicated arrangement and do not show clear profile. Thus, this complication lead possibility that the test was conducted on overlapping collagen fibrils. While imaging of surface topography using fixed tissue is acceptable because fixation with phosphate buffer solution (PBS) will preserve the structural integrity of the tissue, performing mechanical testing on fixed tissue will produce variation of result (Grant et *al*., 2008, Yang et *al*., 2008), because the results revealed the properties of fixed tissue which is not represent of the nature of fresh tissue. In comparison, present study conducting the mechanical testing on fresh frozen tissue without fixing it.

4.2.5. Limitations

There are some shortcomings to the present study. First, the surface topographical imaging was performed in contact mode. When the tip directly probes on the sample surface, the fibrils might be indented and damaged (Heim et *al*., 2006). This behaviour might influence

on the mechanical properties of fibrils in the force spectroscopy test. Secondly, the lack of significant difference in our experimental results probably due to lack of sample size due to the nature of our experimental protocol which require us to wait for 7-8 weeks to get one sample. Thirdly, we merely neglected on the sheep's activities or health prior harvesting skin. As the skin was harvested from the dorsolateral limb, there is possibility that there is newly formed injury on the limb due to the sheep's activities which cannot be traced during surgery. Besides, we also fail to consider about the Langer's line of skin. During AFM testing, the orientation of the skin is not well thought of, hence resulting testing on the collagen fibrils both perpendicular and parallel to Langer's line.

Chapter 5. Conclusion & Future Work

In this study, the elastic properties of sheep expanded skin hierarchical structure at the fibrils and skin tissue were presented. The skin was expanded by anisotropic self-inflating tissue expander developed by OXTEX and implanted at the dorsolateral of right and left limb of Dorper sheep. The properties were compared with normal skin tissue harvested from the same region from different sheep. Based from literatures reported, initially, it is expected that the expanded skin in present study also produced less stiff skin. However this assumption is not supported in the present data.

The nanoindentation testing conducted on the overlap region of the collagen fibrils demonstrated that the elastic modulus of expanded collagen was increased slightly over normal sample. Besides, there was evidence of extension collagen fibrils observed, from the significantly smaller width of collagen fibrils of expanded sample scanned by AFM. This observation is correspond to the qualitative and quantitative data obtained from 3D optical analyser, Alicona which showed that the surface roughness of expanded skin was lower compared to normal skin.

Our results further show that at macrolevel, the elastic modulus obtained from initial region and linear region of expanded skin was also slightly higher compared to normal skin tissue. Besides, the limit strain obtained from the normal skin sample was higher compared to expanded skin, showing that due its higher elasticity, more strain needed to extend the normal skin until failure.

This study demonstrated that due to the expansion, the rearrangement of structural collagen fibrils occurred in order to resist the deformation, thus stretching the collagen fibrils and loosely packed collagen bundles were produced. Therefore, the fibres which are most probably relatively stiff due to the increased of resting tension (from fibrils nanoindentation), resulted in it being more resistant to further stretching (from uniaxial tensile test), thus producing higher moduli at fibril and skin tissue level.

Although some researches supporting that the period of expansion might trigger cellular growth and resulted in new tissue generation, it is not possible to prove this occurrence in present study as concurrent histological study is needed. As present study emphasize of elastic properties of the skin, the other mechanical properties will be further explored in future work. Besides, the mechanical testing performed in present method was tested in ambient condition, thus altering the elastic property of the samples due to dehydration and not representing in vivo condition. Therefore, the future work in this study aims to conduct the nanoindentaion of collagen fibrils and uniaxial tensile test of skin tissue in situ which is by submerging the sample inside water bath of 37^{o}C in order to mimic its in vivo state.

References

Agache, Pierre, Boyer, Jean Pierre, & Laurent, René. (1973). Biomechanical properties and microscopic morphology of human stratum corneum incubated on a wet pad in vitro. *Archiv für dermatologische Forschung, 246*(3), 271-283.

Austad, Eric D, Pasyk, Krystyna A, McClatchey, Kenneth D, & Cherry, George W. (1982). Histomorphologic evaluation of guinea pig skin and soft tissue after controlled tissue expansion. *Plastic and reconstructive surgery, 70*(6), 704-710.

Barbenel, Joseph C, & Evans, JH. (1977). The time-dependent mechanical properties of skin. *Journal of Investigative Dermatology, 69*(3), 318-320.

Bascom, Daphne A, & Wax, Mark K. (2002). Tissue expansion in the head and neck: current state of the art. *Current Opinion in Otolaryngology & Head and Neck Surgery, 10*(4), 273-277.

Bennett, Richard G, & Hirt, Michael. (1993). A history of tissue expansion. *The Journal of dermatologic surgery and oncology, 19*(12), 1066-1073.

Bismuth, Camille, Gerin, Clothilde, Viguier, Eric, Fau, Didier, Dupasquier, Florence, Cavetier, Laurent, . . . Carozzo, Claude. (2014). The biomechanical properties of canine skin measured in situ by uniaxial extension. *Journal of biomechanics*.

Boyer, G., Pailler Mattei, C., Molimard, J., Pericoi, M., Laquieze, S., & Zahouani, H. (2012). Non contact method for in vivo assessment of skin mechanical properties for assessing effect of ageing. *Medical engineering & physics, 34*(2), 172-178.

Cameron, GJ, Alberts, IL, Laing, JH, & Wess, TJ. (2002). Structure of type I and type III heterotypic collagen fibrils: an X-ray diffraction study. *Journal of structural biology, 137*(1), 15-22.

Christensen, MS, Hargens, CW, Nacht, S, & Gans, EH. (1977). Viscoelastic properties of intact human skin: instrumentation, hydration effects, and the contribution of the stratum corneum. *Journal of Investigative Dermatology, 69*(3), 282-286.

Cooper, EUGENE R, Missel, Paul J, Hannon, Daniel P, & Albright, Gregory B. (1985). Mechanical properties of dry, normal, and glycerol-treated skin as measured by the gas-bearing electrodynamometer. *J Soc Cosmet Chem, 36*, 335-348.

Daly, Colin H. (1982). Biomechanical properties of dermis. *Journal of Investigative Dermatology, 79*, 17-20.

Daly, Colin H, & Odland, George F. (1979). Age-related changes in the mechanical properties of human skin. *Journal of Investigative Dermatology, 73*(1), 84-87.

Diridollou, S, Patat, F, Gens, F, Vaillant, L, Black, D, Lagarde, JM, . . . Berson, M. (2000). In vivo model of the mechanical properties of the human skin under suction. *Skin Research and technology, 6*(4), 214-221.

Diridollou, S, Vabre, V, Berson, M, Vaillant, L, Black, D, Lagarde, JM, . . . Patat, F. (2001). Skin ageing: changes of physical properties of human skin in vivo. *International journal of cosmetic science, 23*(6), 353-362.

Edsberg, Laura E, Mates, Robert E, Baier, Robert E, & Lauren, Mark. (1999). Mechanical characteristics of human skin subjected to static versus cyclic normal pressures. *Journal of rehabilitation research and development, 36*(2).

Edwards, Christopher, & Marks, Ronald. (1995). Evaluation of biomechanical properties of human skin. *Clinics in dermatology, 13*(4), 375-380.

Eppell, SJ, Smith, BN, Kahn, H, & Ballarini, R. (2006). Nano measurements with micro-devices: mechanical properties of hydrated collagen fibrils. *Journal of the Royal Society Interface, 3*(6), 117-121.

Ersek, RA, & Vazquez-Salisbury, A. (1994). Wound closure using a skin stretching device. *Contemporary orthopaedics, 28*(6), 495-500.

Finlay, B. (1969). Scanning electron microscopy of the human dermis under uni-axial strain. *Biomedical engineering, 4*(7), 322.

Fleury, Vincent, Al-Kilani, Alia, Boryskina, Olena P, Cornelissen, Annemiek JM, Nguyen, Thi-Hanh, Unbekandt, Mathieu, . . . Sire, Olivier. (2010). Introducing the scanning air puff tonometer for biological studies. *Physical Review E, 81*(2), 021920.

Flynn, Cormac, Taberner, Andrew, & Nielsen, Poul. (2011). Mechanical characterisation of in vivo human skin using a 3D force-sensitive micro-robot and finite element analysis. *Biomechanics and modeling in mechanobiology, 10*(1), 27-38.

Fratzl, Peter, Misof, Klaus, Zizak, Ivo, Rapp, Gert, Amenitsch, Heinz, & Bernstorff, Sigrid. (1998). Fibrillar structure and mechanical properties of collagen. *Journal of structural biology, 122*(1), 119-122.

Fujimura, Tsutomu, Osanai, Osamu, Moriwaki, Shigeru, Akazaki, Syuichi, & Takema, Yoshinori. (2008). Development of a novel method to measure the elastic properties of skin including subcutaneous tissue: New age-related parameters and scope of application. *Skin Research and Technology, 14*(4), 504-511.

Graham, Helen K, Hodson, Nigel W, Hoyland, Judith A, Millward-Sadler, Sarah J, Garrod, David, Scothern, Anthea, . . . Erler, Janine T. (2010). Tissue section AFM: In situ ultrastructural imaging of native biomolecules. *Matrix Biology, 29*(4), 254-260.

Graham, John S, Vomund, Anthony N, Phillips, Charlotte L, & Grandbois, Michel. (2004). Structural changes in human type I collagen fibrils investigated by force spectroscopy. *Experimental cell research, 299*(2), 335-342.

Grant, Colin A, Brockwell, David J, Radford, Sheena E, & Thomson, Neil H. (2008). Effects of hydration on the mechanical response of individual collagen fibrils. *Applied Physics Letters, 92*(23), 233902.

Gutsmann, Thomas, Fantner, Georg E, Kindt, Johannes H, Venturoni, Manuela, Danielsen, Signe, & Hansma, Paul K. (2004). Force spectroscopy of collagen fibers to investigate their mechanical properties and structural organization. *Biophysical journal, 86*(5), 3186-3193.

Heim, August J, Matthews, William G, & Koob, Thomas J. (2006). Determination of the elastic modulus of native collagen fibrils via radial indentation. *Applied physics letters, 89*(18), 181902.

Hendriks, FM. (1969). Mechanical behaviour of human skin in vivo. *Bio-medical Engineering, 4*, 322-327.

Holt, Brian, Tripathi, Anubhav, & Morgan, Jeffrey. (2008). Viscoelastic response of human skin to low magnitude physiologically relevant shear. *Journal of biomechanics, 41*(12), 2689-2695.

Holzapfel, Gerhard A. (2001). Biomechanics of soft tissue. *The handbook of materials behavior models, 3*, 1049-1063.

Hulmes, DJ, Wess, Tim J, Prockop, Darwin J, & Fratzl, Peter. (1995). Radial packing, order, and disorder in collagen fibrils. *Biophysical Journal, 68*(5), 1661-1670.

Janko, Marek, Zink, Albert, Gigler, Alexander M, Heckl, Wolfgang M, & Stark, Robert W. (2010). Nanostructure and mechanics of mummified type I collagen from the 5300-year-old Tyrolean Iceman. *Proceedings of the Royal Society B: Biological Sciences, 277*(1692), 2301-2309.

Jastrzebska, M, Barwinski, B, Mroz, I, Turek, A, Zalewska-Rejdak, J, & Cwalina, B. (2005). Atomic force microscopy investigation of chemically stabilized pericardium tissue. *The European Physical Journal E, 16*(4), 381-388.

Kasas, S, Thomson, NH, Smith, BL, Hansma, PK, Miklossy, J, & Hansma, HG. (1997). Biological applications of the AFM: from single molecules to organs. *International Journal of Imaging Systems and Technology, 8*(2), 151-161.

Kennedy, Craig J, & Wess, Tim J. (2003). The structure of collagen within parchment–a review. *Restaurator, 24*(2), 61-80.

Khatyr, Fouad, Imberdis, Claude, Varchon, Daniel, Lagarde, Jean-Michel, & Josse, Gwendal. (2006). Measurement of the mechanical properties of the skin using the suction test. *Skin research and technology, 12*(1), 24-31.

Langer, K. (1978). On the anatomy and physiology of the skin: I. The cleavability of the cutis. *British journal of plastic surgery, 31*(1), 3-8.

Leite, FL, Mattoso, LHC, Oliveira Junior, ON, & Herrmann Junior, PSP. (2007). The Atomic Force Spectroscopy as a Tool to Investigate Surface Forces: Basic Principles and Applications. *Méndez-Vilas A and Díaz J. Modern Research and Educational Topics in Microscopy. Formatex*, 747-757.

Li, Xinhui, Ji, Tong, Hu, Jun, & Sun, Jielin. (2008). Optimization of specimen preparation of thin cell section for AFM observation. *Ultramicroscopy, 108*(9), 826-831.

Liu, Z, & Yeung, K. (2008). The preconditioning and stress relaxation of skin tissue. *Journal of Biomedical & Pharmaceutical Engineering, 2*(1), 22-28.

Marcus, Jeffrey, Horan, Douglas B, & Robinson, June K. (1990). Tissue expansion: past, present, and future. *Journal of the American Academy of Dermatology, 23*(5), 813-825.

Marks, R. (2004). The stratum corneum barrier: the final frontier. *The Journal of nutrition, 134*(8), 2017S-2021S.

Matsko, Nadezda, & Mueller, Martin. (2004). AFM of biological material embedded in epoxy resin. *Journal of structural biology, 146*(3), 334-343.

McGrath, JA, Eady, RAJ, & Pope, FM. (2010). Anatomy and organization of human skin. *Rook's textbook of dermatology, 1*.

Minary-Jolandan, Majid, & Yu, Min-Feng. (2009). Nanomechanical heterogeneity in the gap and overlap regions of type I collagen fibrils with implications for bone heterogeneity. *Biomacromolecules, 10*(9), 2565-2570.

Mosler, E, Folkhard, W, Knörzer, E, Nemetschek-Gansler, H, Nemetschek, Th, & Koch, MHJ. (1985). Stress-induced molecular rearrangement in tendon collagen. *Journal of molecular biology, 182*(4), 589-596.

Munoz, MJ, Bea, JA, Rodríguez, JF, Ochoa, I, Grasa, J, Pérez del Palomar, A, . . . Doblaré, M. (2008). An experimental study of the mouse skin behaviour: Damage and inelastic aspects. *Journal of biomechanics, 41*(1), 93-99.

Neumann, Charles G. (1957). The expansion of an area of skin by progressive distention of a subcutaneous balloon: use of the method for securing skin for subtotal reconstruction of the ear. *Plastic and reconstructive surgery, 19*(2), 124-130.

Ní Annaidh, Aisling, Bruyère, Karine, Destrade, Michel, Gilchrist, Michael D, & Otténio, Mélanie. (2012). Characterization of the anisotropic mechanical properties of excised human skin. *Journal of the Mechanical Behavior of Biomedical Materials, 5*(1), 139-148.

Pailler-Mattei, C, & Zahouani, H. (2004). Study of adhesion forces and mechanical properties of human skin in vivo. *Journal of adhesion science and technology, 18*(15-16), 1739-1758.

Pailler-Mattei, C., Bec, S., & Zahouani, H. (2008). In vivo measurements of the elastic mechanical properties of human skin by indentation tests. *Medical Engineering & Physics, 30*(5), 599-606.

Pamplona, Djenane C, Velloso, Raquel Q, & Radwanski, Henrique N. (2014). On skin expansion. *Journal of the mechanical behavior of biomedical materials, 29*, 655-662.

Puxkandl, R, Zizak, I, Paris, O, Keckes, J, Tesch, W, Bernstorff, S, . . . Fratzl, P. (2002). Viscoelastic properties of collagen: synchrotron radiation investigations and structural model. *Philosophical Transactions of the Royal Society of London. Series B: Biological Sciences, 357*(1418), 191-197.

Sanders, Joan E, Goldstein, Barry S, & Leotta, Daniel F. (1995). Skin response to mechanical stress: adaptation rather than breakdown-a review of the literature. *Journal of rehabilitation research and development, 32*, 214-214.

Schneider, Marc S, Borkow, Joel E, Cruz, Ildefonso T, Marangoni, Roy D, Shaffer, Janice, & Grove, Dan. (1988). The tensiometric properties of expanded guinea pig skin. *Plastic and reconstructive surgery, 81*(3), 398-403.

Shen, Zhilei Liu, Kahn, Harold, Ballarini, Roberto, & Eppell, Steven J. (2011). Viscoelastic properties of isolated collagen fibrils. *Biophysical journal, 100*(12), 3008-3015.

Shergold, Oliver A, Fleck, Norman A, & Radford, Darren. (2006). The uniaxial stress versus strain response of pig skin and silicone rubber at low and high strain rates. *International Journal of Impact Engineering, 32*(9), 1384-1402.

Sopher, Ran, & Gefen, Amit. (2011). Effects of skin wrinkles, age and wetness on mechanical loads in the stratum corneum as related to skin lesions. *Medical & biological engineering & computing, 49*(1), 97-105.

Squier, Christopher A. (1980). The Stretching of Mouse Skin in Vivo: Effect on Epidermal Proliferation and Thickness. *Journal of Investigative Dermatology, 74*(2).

Strasser, Stefan, Zink, Albert, Janko, Marek, Heckl, Wolfgang M, & Thalhammer, Stefan. (2007). Structural investigations on native collagen type I fibrils using AFM. *Biochemical and biophysical research communications, 354*(1), 27-32.

Svensson, René B, Hansen, Philip, Hassenkam, Tue, Haraldsson, Bjarki T, Aagaard, Per, Kovanen, Vuokko, Magnusson, S Peter. (2012). Mechanical properties of human

patellar tendon at the hierarchical levels of tendon and fibril. *Journal of Applied Physiology, 112*(3), 419-426.

Swan, Marc C, Bucknall, David G, Czernuszka, Jan T, Pigott, David W, & Goodacre, Timothy EE. (2012). Development of a Novel Anisotropic Self-Inflating Tissue Expander: In Vivo Submucoperiosteal Performance in the Porcine Hard Palate. *Plastic and reconstructive surgery, 129*(1), 79-88.

Swan, MC, Bucknall, DG, Goodacre, TEE, & Czernuszka, JT. (2011). Synthesis and properties of a novel anisotropic self-inflating hydrogel tissue expander. *Acta biomaterialia, 7*(3), 1126-1132.

Timmenga, Erik JF, Schoorl, Reinier, & Klopper, Pieter J. (1990). Biomechanical and histomorphological changes in expanded rabbit skin. *British journal of plastic surgery, 43*(1), 101-106.

Wen, C-Y, Wu, C-B, Tang, B, Wang, T, Yan, C-H, Lu, WW, Chiu, K-Y. (2012). Collagen fibril stiffening in osteoarthritic cartilage of human beings revealed by atomic force microscopy. *Osteoarthritis and Cartilage, 20*(8), 916-922.

Wenger, Marco PE, Bozec, Laurent, Horton, Michael A, & Mesquida, Patrick. (2007). Mechanical properties of collagen fibrils. *Biophysical journal, 93*(4), 1255-1263.

Wildnauer, Richard H, Bothwell, James W, & Douglass, Alexander B. (1971). Stratum corneum biomechanical properties I. Influence of relative humidity on normal and extracted human stratum corneum. *Journal of Investigative Dermatology, 56*(1), 72-78.

Wilhelmi, Brad J, Blackwell, Steven J, Mancoll, John S, & Phillips, Linda G. (1998). Creep vs. stretch: a review of the viscoelastic properties of skin. *Annals of plastic surgery, 41*(2), 215-219.

Wilkes, GL, Brown, IA, & Wildnauer, RH. (1973). The biomechanical properties of skin. *CRC critical reviews in bioengineering, 1*(4), 453.

Wilkinson, SJ, & Hukins, DWL. (1999). Determination of collagen fibril structure and orientation in connective tissues by X-ray diffraction. *Radiation Physics and Chemistry, 56*(1), 197-204.

Wu, Kenneth S, van Osdol, William W, & Dauskardt, Reinhold H. (2006). Mechanical properties of human stratum corneum: effects of temperature, hydration, and chemical treatment. *Biomaterials, 27*(5), 785-795.

Yang, Lanti, Van der Werf, Kees O, Fitié, Carel FC, Bennink, Martin L, Dijkstra, Pieter J, & Feijen, Jan. (2008). Mechanical properties of native and cross-linked type I collagen fibrils. *Biophysical journal, 94*(6), 2204-2211.

Zahouani, H, Pailler-Mattei, C, Sohm, B, Vargiolu, R, Cenizo, V, & Debret, R. (2009). Characterization of the mechanical properties of a dermal equivalent compared with human skin in vivo by indentation and static friction tests. *Skin research and technology, 15*(1), 68-76.

ŻAK, MALGORZATA, Kuropka, Piotr, Kobielarz, Magdalena, Dudek, Agnieszka, Kaleta-Kuratewicz, Katarzyna, & Szotek, Sylwia. (2011). Determination of the mechanical properties of the skin of pig foetuses with respect to its structure. *Acta of Bioengineering & Biomechanics, 13*(2).

Zeng, Yan-jun, Liu, Yu-hong, Xu, Chuan-qing, Xu, Xiao-hu, Xu, Hong, & Sun, Guang-ci. (2004). Biomechanical properties of skin in vitro for different expansion methods. *Clinical Biomechanics*, *19*(8), 853-857.

Zhang, En-ping, Liao, Dong-hua, Liu, Ai-zhen, Wang, Xiao-bing, Li, Xiao-yang, Zeng, Yan-jun, & Wang, Su-jie. (2006). Biomechanical characteristics investigation on long-term free graft with expanded porcine skin. *Clinical Biomechanics*, *21*(8), 864-869.

APPENDIX A

Independent 2 sample t-test for z-height

Group Statistics					
	zheight	N	Mean	Std. Deviation	Std. Error Mean
Vzheight	Control	6	28.6967	6.01842	2.45701
	Expanded	4	14.3625	5.18651	2.59326

	Levene's Test for Equality of Variances		t-test for Equality of						
		Sig.	t	df	Sig. (2-tailed)	Mean Difference	Std. Error Difference	95% Confidence Interval of the	
								Lower	Upper
Vzheight	Equal variances assumed						3.69266	5.81887	22.84946
	Equal variances not assumed		4.013	7.283	0.005	14.33417	3.57238	5.95282	22.71552

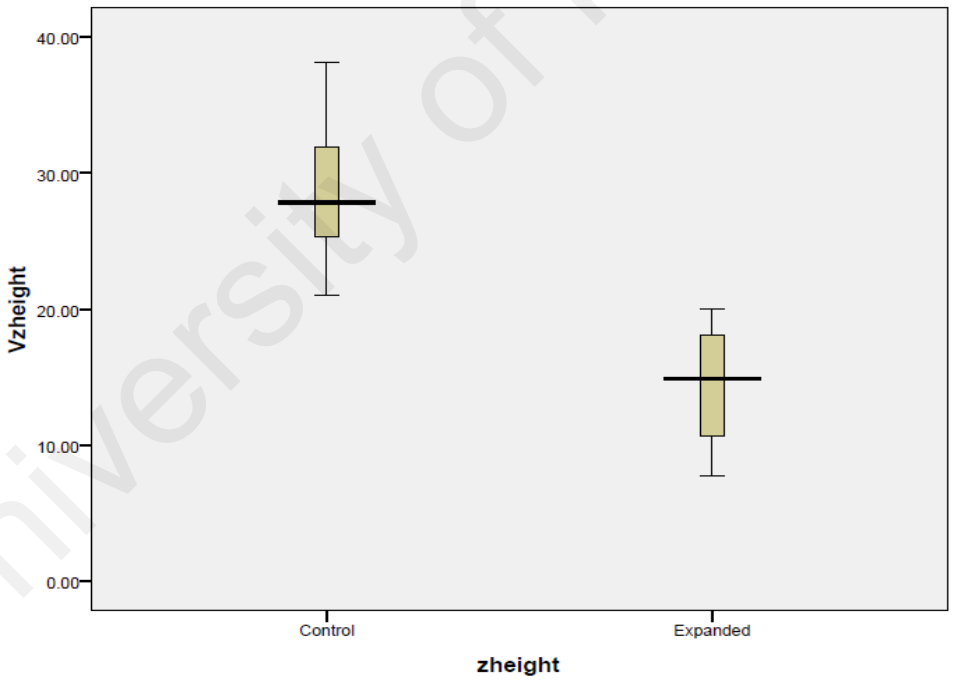

APPENDIX B

Independent 2 sample t-test for Sa

Group Statistics					
	Sa	N	Mean	Std. Deviation	Std. Error Mean
VSa	Control	6	6.335	1.17151	0.47827
	Expanded	4	3.1625	1.62518	0.81259

Independent Samples Test										
		Levene's Test for Equality of Variances		t-test for Equality of						
			Sig.	t	df	Sig. (2-tailed)	Mean Difference	Std. Error Difference	95% Confidence Interval of the	
									Lower	Upper
VSa	Equal variances assumed							0.87755	1.14886	5.19614
	Equal variances not assumed			3.365	5.073	0.02	3.1725	0.94289	0.7592	5.5858

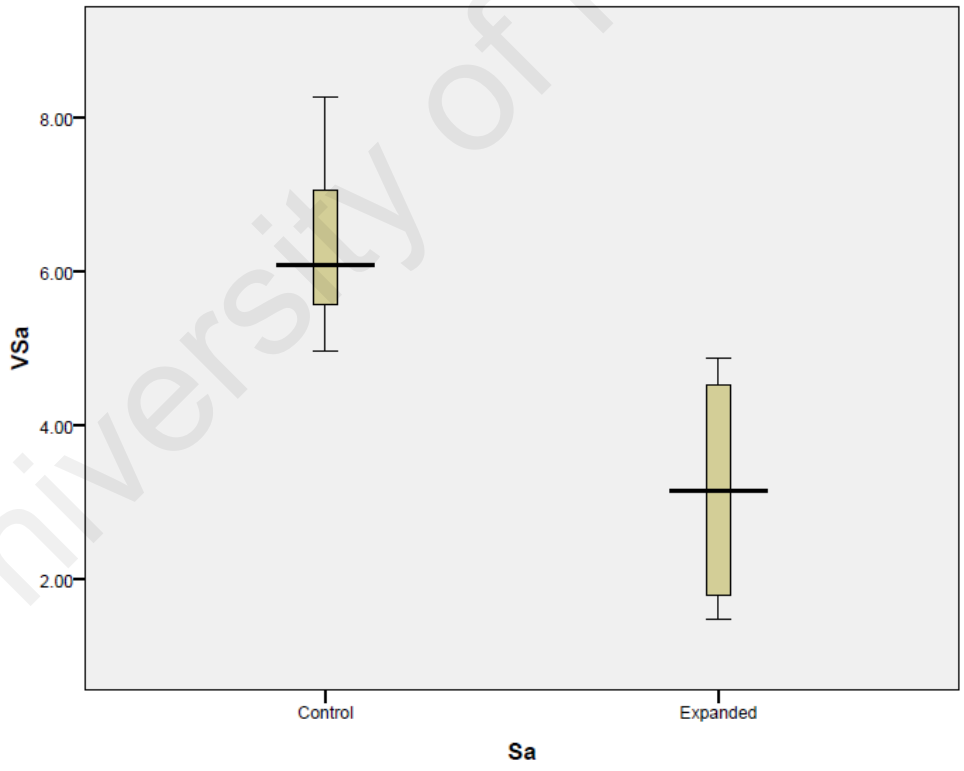

APPENDIX C

Independent 2 sample t-test for Ra

Group Statistics					
	Ra	N	Mean	Std. Deviation	Std. Error Mean
VRa	Control	6	1.4217	0.6449	0.26328
	Expanded	4	0.5525	0.26336	0.13168

Independent Samples Test										
		Levene's Test for Equality of Variances		t-test for Equality of						
			Sig.	t	df	Sig. (2-tailed)	Mean Difference	Std. Error Difference	95% Confidence Interval of the	
									Lower	Upper
VRa	Equal variances assumed							0.34517	0.0732	1.66513
	Equal variances not assumed			2.953	7.076	0.021	0.86917	0.29437	0.1746	1.56373

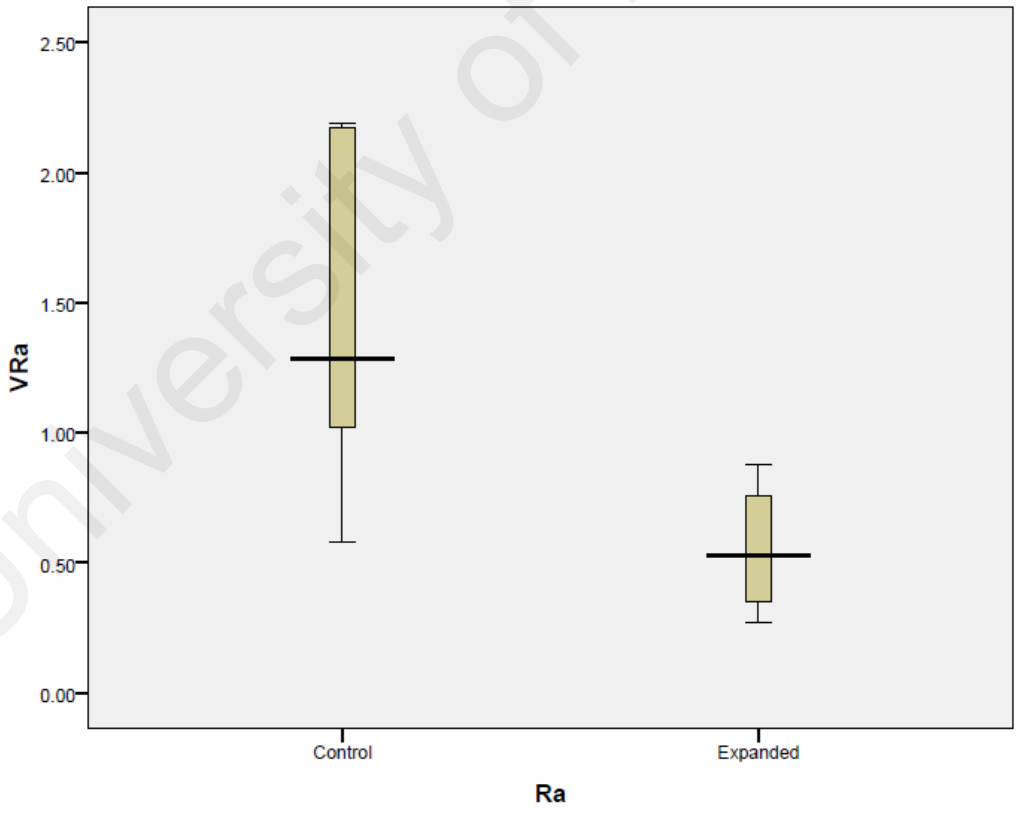

APPENDIX D

Independent 2 sample t-test for AFM D-banding

Group Statistics					
	D	N	Mean	Std. Deviation	Std. Error Mean
VD	Control	28	63.511786	2.57424574	0.48648672
	Expanded	26	63.711538	2.67897098	0.52538944

Independent Samples Test										
		Levene's Test for Equality of Variances		t-test for Equality of						
			Sig.	t	df	Sig. (2-tailed)	Mean Difference	Std. Error Difference	95% Confidence Interval of the	
									Lower	Upper
VD	Equal variances assumed							0.7149566	-1.63441812	1.23491262
	Equal variances not assumed			-0.279	51.317	0.781	-0.19975275	0.71603309	-1.63703326	1.23752777

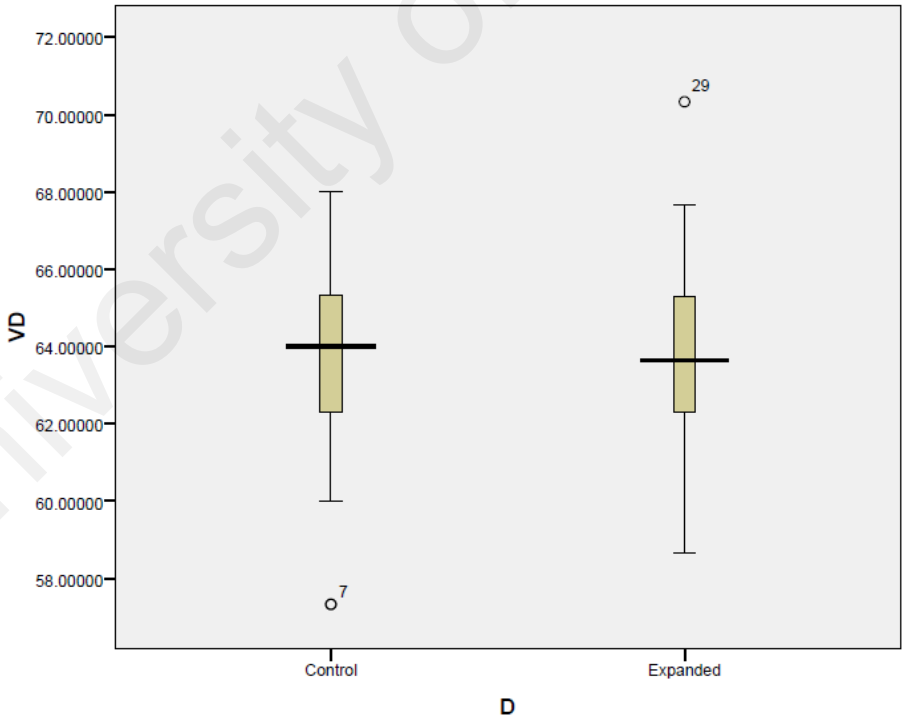

APPENDIX E

Independent 2 sample t-test for AFM Width

Group Statistics					
	Width	N	Mean	Std. Deviation	Std. Error Mean
VWidth	Control	11	153.91	25.3474	7.64253
	Expanded	11	106.7	28.48737	8.58926

Independent Samples Test										
		Levene's Test for Equality of Variances		t-test for Equality of						
			Sig.	t	df	Sig. (2-tailed)	Mean Difference	Std. Error Difference	95% Confidence Interval of the	
									Lower	Upper
VWidth	Equal variances assumed							11.49712	23.22652	71.19166
	Equal variances not assumed			4.106	19.733	0.001	47.20909	11.49712	23.20573	71.21246

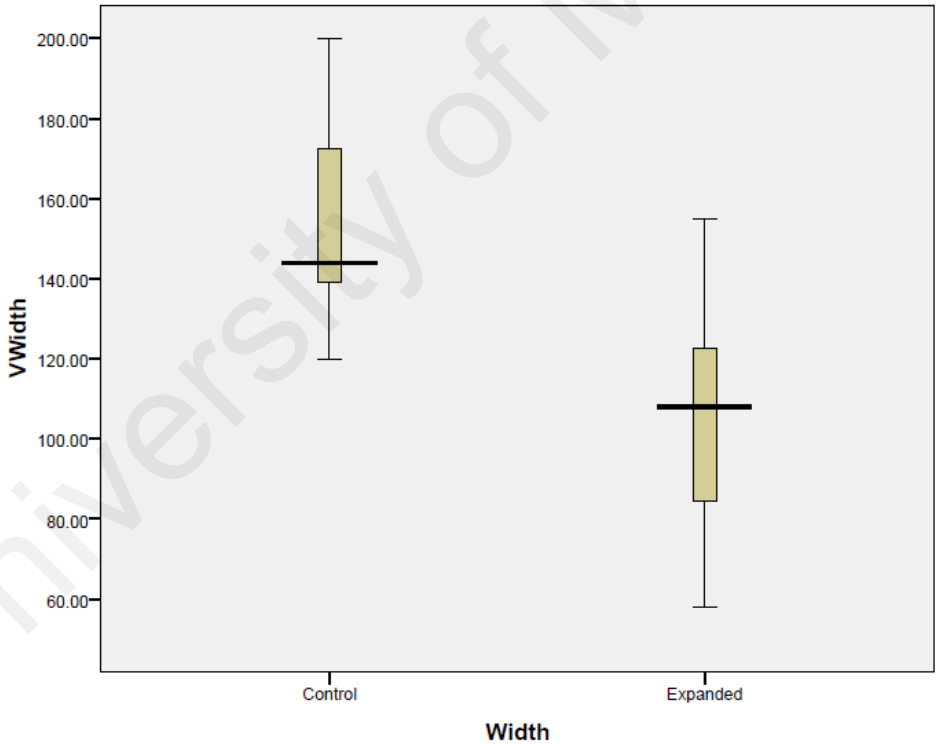

APPENDIX F

Independent 2 sample t-test for AFM Force Spectroscopy

Group Statistics					
	AFM	N	Mean	Std. Deviation	Std. Error Mean
VAFM	Control	57	36.14067	29.52375886	3.91051739
	Expanded	48	45.932646	24.08873282	3.47690909

Independent Samples Test										
		Levene's Test for Equality of Variances		t-test for Equality of						
			Sig.	t	df	Sig. (2-tailed)	Mean Difference	Std. Error Difference	95% Confidence Interval of the	
									Lower	Upper
VAFM	Equal variances assumed							5.32436411	-20.3515961	0.76764478
	Equal variances not assumed			-1.871	102.909	0.064	-9.79197566	5.23268986	-20.16989079	0.5859394

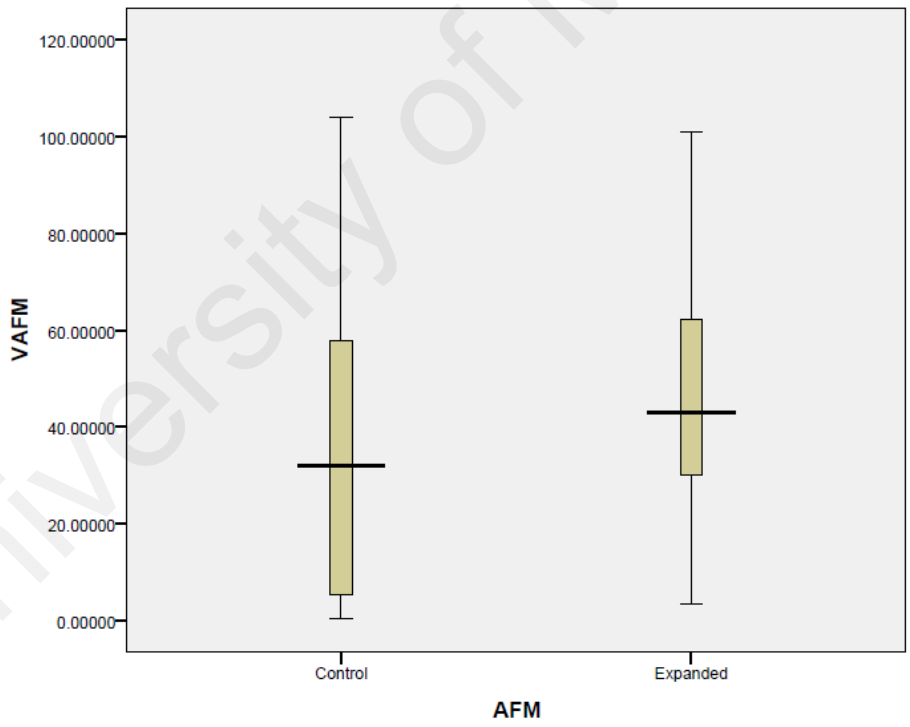

APPENDIX G

Independent 2 sample t-test for E_0

Group Statistics					
	E1	N	Mean	Std. Deviation	Std. Error Mean
VE1	Control	5	0.2694649	0.19165442	0.08571046
	Expanded	5	0.8497653	0.6749132	0.30183036

Independent Samples Test										
		Levene's Test for Equality of Variances		t-test for Equality of						
			Sig.	t	df	Sig. (2-tailed)	Mean Difference	Std. Error Difference	95% Confidence Interval of the	
									Lower	Upper
VE1	Equal variances assumed							0.313764	-1.30384144	0.14324073
	Equal variances not assumed			-1.849	4.641	0.128	-0.58030036	0.313764	-1.40599175	0.2453910

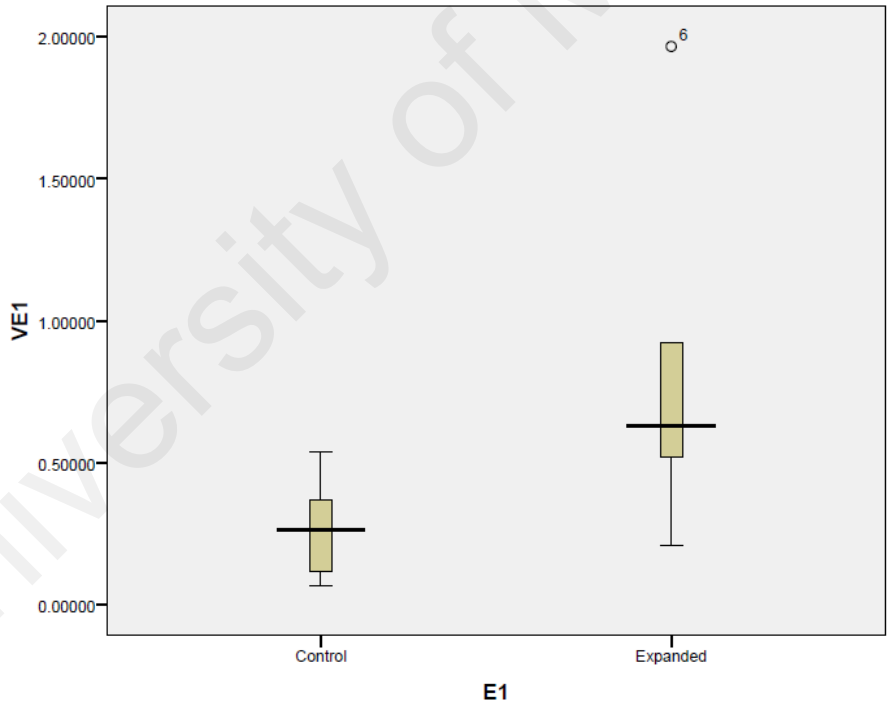

APPENDIX H

Independent 2 sample t-test for E_{∞}

Group Statistics					
	E2	N	Mean	Std. Deviation	Std. Error Mean
VE2	Control	5	1.9755556	1.64880054	0.73736602
	Expanded	5	4.402184	1.96948724	0.88078147

Independent Samples Test										
		Levene's Test for Equality of Variances		t-test for Equality of						
			Sig.	t	df	Sig. (2-tailed)	Mean Difference	Std. Error Difference	95% Confidence Interval of the	
									Lower	Upper
VE2	Equal variances assumed							1.14868823	-5.07550827	0.22225133
	Equal variances not assumed			-2.113	7.76	0.069	-2.42662847	1.14868823	-5.08983857	0.23658163